



HHS Public Access

Author manuscript

Biol Psychiatry Cogn Neurosci Neuroimaging. Author manuscript; available in PMC 2023 September 01.

Published in final edited form as:

Biol Psychiatry Cogn Neurosci Neuroimaging. 2022 September ; 7(9): 935–948. doi:10.1016/j.bpsc.2022.02.008.

Remodeling of the Cortical Structural Connectome in Posttraumatic Stress Disorder: Results from the ENIGMA-PGC PTSD Consortium

A full list of authors and affiliations appears at the end of the article.

Abstract

Background: Posttraumatic stress disorder (PTSD) is accompanied by disrupted cortical neuroanatomy. We investigated alteration in covariance of structural networks associated with PTSD in regions that demonstrate the case-control differences in cortical thickness (CT) and surface area (SA).

Methods: Neuroimaging and clinical data were aggregated from 29 research sites in >1,300 PTSD cases and >2,000 trauma-exposed controls (age 6.2–85.2 years) by the ENIGMA-PGC PTSD working group. Cortical regions in the network were rank-ordered by effect size of PTSD-related cortical differences in CT and SA. The top- n ($n = 2$ to 148) regions with the largest between-group differences in effect size for PTSD > non-PTSD formed *hypertrophic networks*, the largest effect size for PTSD < non-PTSD formed *atrophic networks*, and the smallest effect size of between-group differences formed *stable networks*. The mean structural covariance (SC) of a given n -region network was the average of all positive pairwise correlations and was compared to the mean SC of 5,000 randomly generated n -region networks. For methodologic confirmation we demonstrated that PTSD patients had higher mean SC as compared to random networks in CT-based and SA-based atrophic networks, CT-based and SA-based hypertrophic networks, and CT-based stable networks. We also confirmed that non-PTSD participants showed higher mean SC

*Corresponding Author: Rajendra A. Morey, M.D., 40 Duke Medicine Circle, Room 414, Durham, NC 27710 USA, Phone: 919-286-0411 ext. 6425, Facsimile: 919-416-5912, rajendra.morey@duke.edu.

Conflicts of Interest

Dr. Abdallah has served as a consultant, speaker and/or on advisory boards for FSV7, Lundbeck, Psilocybin Labs, Genentech and Janssen, and editor of Chronic Stress for Sage Publications, Inc.; he has filed a patent for using mTOR inhibitors to augment the effects of antidepressants (filed on August 20, 2018). Dr. Davidson is the founder and president of, and serves on the board of directors for, the non-profit organization Healthy Minds Innovations, Inc. Dr. Jahanshad received partial research support from Biogen, Inc. (Boston, USA) for research unrelated to the content of this manuscript. Dr. Krystal is a consultant for AbbVie, Inc., Amgen, Astellas Pharma Global Development, Inc., AstraZeneca Pharmaceuticals, Biomedisyn Corporation, Bristol-Myers Squibb, Eli Lilly and Company, Euthymics Bioscience, Inc., Neurovance, Inc., FORUM Pharmaceuticals, Janssen Research & Development, Lundbeck Research USA, Novartis Pharma AG, Otsuka America Pharmaceutical, Inc., Sage Therapeutics, Inc., Sunovion Pharmaceuticals, Inc., and Takeda Industries; is on the Scientific Advisory Board for Lohocla Research Corporation, Mnemosyne Pharmaceuticals, Inc., Naurex, Inc., and Pfizer; is a stockholder in Biohaven Pharmaceuticals; holds stock options in Mnemosyne Pharmaceuticals, Inc.; holds patents for Dopamine and Noradrenergic Reuptake Inhibitors in Treatment of Schizophrenia, US Patent No. 5,447,948 (issued September 5, 1995), and Glutamate Modulating Agents in the Treatment of Mental Disorders, U.S. Patent No. 8,778,979 (issued July 15, 2014); and filed a patent for Intranasal Administration of Ketamine to Treat Depression. U.S. Application No. 14/197,767 (filed on March 5, 2014); US application or Patent Cooperation Treaty international application No. 14/306,382 (filed on June 17, 2014). Filed a patent for using mTOR inhibitors to augment the effects of antidepressants (filed on August 20, 2018). Dr. Schmahl is consultant for Boehringer Ingelheim International GmbH. Dr. Stein has received research grants and/or consultancy honoraria from Lundbeck and Sun. Dr. Thompson received partial research support from Biogen, Inc. (Boston, USA) for research unrelated to the topic of this manuscript. All other authors have no conflicts of interest to declare.

than random networks in CT-based and SA-based atrophic networks, and SA-based hypertrophic networks.

Results: Patients with PTSD, relative to non-PTSD controls, exhibited lower mean SC in CT-based and SA-based atrophic networks. Patients with PTSD alone showed lower mean SC in CT-based atrophic networks than patients with depression alone, and higher mean SC in SA-based atrophic networks than PTSD patients with comorbid depression as well as healthy controls. Sex and age modulated covariance differences of PTSD-related structural networks.

Conclusions: Covariance of structural networks based on CT and cortical SA are affected by PTSD and further modulated by comorbid depression, sex, and age. The structural covariance networks that are perturbed in PTSD comport with converging evidence from resting state functional connectivity networks and networks impacted by inflammatory processes, and stress hormones in PTSD.

Keywords

PTSD; Cortical Thickness; Surface Area; Structural Covariance; Brain Network; Depression

Introduction

Posttraumatic stress disorder (PTSD) is a psychiatric condition that develops in vulnerable individuals after experiencing or witnessing a life-threatening event (1). PTSD-related changes in cortical thickness (CT) (2–5) and surface area (SA) (6, 7) are found in specific cortical regions. However, relatively little is known about how PTSD affects coordinated patterns of CT and SA differences among affected cortical regions. We sought to examine PTSD effects on networks made up of cortical regions that have the greatest and the least between-group differences in CT and SA. Identifying such networks may lend support for one or more etiopathologic models of PTSD.

Structural covariance (SC) refers to the phenomenon of covarying structural brain imaging measures between cortical regions and across individuals. This covariance may be instantiated as a structural covariance network (SCN). Structural covariance network measures are shown to be concordant with tract-based white matter connectivity, synchronous neuronal activity (e.g. functional connectivity) (8, 9), and spatial patterns of gene transcription, each of which lend biological support to SCNs (10). SCNs may index mutually trophic factors between regions that covary over the course of neurodevelopment (9). Differences in SC are associated with a variety of neuropsychiatric disorders including PTSD (11–13), schizophrenia, autism, obsessive compulsive disorder (14, 15), and even trauma exposure (16).

Our investigation of structural networks with significantly different covariance was motivated by two complementary models for understanding PTSD. **(I)** There is converging evidence that neurobiological mechanisms drive concerted patterns (covariance) of atrophy or hypertrophy across selected brain regions. There is generally more evidence supporting a role for CT-derived networks than SA-derived networks. Concerted processes operative in healthy neurobiological states are perturbed by disease to effect patterns of network

atrophy or hypertrophy. These neurobiological perturbations may manifest as changes in network covariance. Neurobiologically deleterious processes in PTSD may instigate atrophy in a coordinated manner across many regions to reveal *atrophic* networks. Deleterious processes in PTSD include chronic alteration of stress hormone levels such as cortisol and norepinephrine (17, 18), epigenetics mechanisms such as methylation (19, 20), inflammatory processes such as oxidative stress (21) and cytokines (22), and accelerated aging through the combined effect of these and other processes (23). **(II)** Alternatively, between-group differences in network SC may support one or the other prevailing neural systems models of PTSD. For instance, a dominant model of PTSD is that fear learning systems go awry in the aftermath of trauma. Behaviorally, slow or incomplete fear extinction and rapid fear-reinstatement contribute to symptoms of PTSD. Effective fear learning is dependent on the healthy function of underlying brain networks. Functional connectivity networks have been found to be congruent with structural covariance networks (24, 25). Thus, between-group differences in structural networks may simply reflect the between-group differences in functional networks, and these differences pervade networks (structural and functional) involved in fear learning behavior. It is also possible we might find hypertrophy across different networks that mediate compensatory responses to disrupted fear learning.

Wannan and colleagues (26) pioneered an innovative method to investigate the mean SC of networks constituted from regions selected by rank-ordering regions most affected by the illness of interest. This method considers only the most highly ranked regions in forming networks rather than all regions as in previous SCN analyses. Their findings in schizophrenia, suggest that some cortical networks *connecting* diverse regions may propagate cortical features from one region to another, leading to distributed cortical remodeling (9). Our approach, which modified their method, considered 3 classes of networks. (I) regions most affected by virtue of lower CT in PTSD formed so-called *atrophic networks*. (II) Regions most affected by virtue of higher CT in PTSD formed so-called *hypertrophic networks*. (III) Regions least affected by PTSD formed *stable networks*. Rank-ordering of regions was based on the effect size of between group differences in CT or SA. The threshold for considering effect sizes (top-n) was initially set to the 2-most affected regions, and was repeated for networks of up to 148 regions (top-n = 2, 3, 4, . . . 148). Thus, networks ranging in size from 2 to 148 regions, in increments of 1 region, were tested. The SC of a network was calculated as the average effect size of the regions under consideration.

Importantly, even in the absence of statistically significant group-differences for individual cortical regions, significant group differences in covariance were detected in networks consisting of regions with the greatest between-group differences. We examined both CT-based and SA-based networks because CT and SA index distinct features of neuronal organization (27–29). This approach enhanced sensitivity to cortical morphometry and network covariance differences associated with PTSD, given that CT- and SA-based networks may reflect different interactions between regions or distinct aspects of the same interaction between regions (30, 31). Cortical volume was not examined as it is readily derived from mean CT and SA by simple multiplication of these two terms. However, CT

and SA possess different biological, developmental, and genetic determinants as we discuss later.

We hypothesized that the mean covariance of n -region networks would be higher than the mean covariance of randomly selected n -region networks in both PTSD and trauma-exposed control groups. Confirmation of this hypothesis would tell us that networks constituted from selected (top- n) regions are more structurally interconnected than networks of the same size composed of randomly selected regions. We further hypothesized that mean SC would be modulated by PTSD diagnosis, as well as by PTSD and comorbid depression, given the two disorders are highly comorbid (32). Confirmation of this hypothesis would demonstrate that the interconnectedness of the network regions (top- n) is significantly altered in PTSD. We predicted greater impact of PTSD on SA-based networks than on CT-based networks because SA generally drives performance more directly for a variety of cognitive and affective processes (33, 34). We also know that SA has an outsized role compared to CT in various neurobiological, neurodevelopmental, and neurogenetic processes. We predicted, because stable networks are made of regions that are least affected by PTSD, their covariance might be stronger than in non-PTSD since these networks of the least affected regions might compensate for disrupted networks composed of highly affected regions. We posited that because atrophic networks are made of regions most diminished by illness, the disease process would not necessarily affect all network regions in a systematic way, effectively lowering covariance. By contrast, we predicted that trauma-exposed non-PTSD subjects might be protected from developing symptoms because their atrophic networks maintained their healthy level of covariance. If hypertrophic networks result from higher-than-normal levels of trophic factors, whereas atrophic networks result from lower-than-normal levels of trophic factors, then we might reason that atrophic and hypertrophic networks would experience the same perturbations. However, given evidence that stress hormones and inflammatory processes play a role in regional atrophy but a lack of evidence for a role in regional hypertrophic, we predicted that hypertrophic networks would demonstrate different outcomes in relation to PTSD than atrophic networks. Specifically, we hypothesized that atrophic networks, unlike hypertrophic networks, would play a central role in modulating the effects of PTSD. Finally, we explored interaction effects of sex, age, and depression on PTSD.

Methods

Participants

All data, aggregated by the PGC-ENIGMA PTSD Working Group, was shared by 29 sites located in five countries ($N=3,438$ for CT, and 3,436 for SA). Demographic and clinical information are summarized in Table 1. Only participants with clear information of PTSD diagnosis and sex were included in the following analyses (PTSD/Non-PTSD $N=1,344/2,073$ for CT, and 1,348/2,066 for SA). The specific psychometric instruments and MRI acquisition parameters used at each study site are listed in Supplementary Tables S1 and S2, respectively. Most sites used clinician-administered measures such as the Structured Clinical Interview for DSM (SCID) (35) or Clinician-Administered PTSD Scale (CAPS) (36, 37) to ascertain PTSD diagnosis. The majority used DSM-IV criteria, but a small

subset of sites used DSM-5 criteria. Severity of PTSD symptoms was derived from the same measures used for diagnosis, except when a clinician-administered measure (e.g., SCID) lacked severity information (see Supplementary Table S1). The measures reflect PTSD diagnosis and symptoms in the month before scanning. Sites used a mix of clinician-administered and self-report instruments to diagnose depression. We harmonized depression data by assigning participants to major depressive disorder (MDD) or control groups based on a standardized depression severity cut-off score. Most sites reported depression severity using the Beck Depression Inventory-II (BDI-II) (38), while other scales included the Center for Epidemiologic Studies Depression Scale (CES-D) (39), Hamilton Depression Rating Scale (HAM-D) (40, 41), Depression Anxiety Stress Scales (DASS) (42), and Children's Depression Inventory (CDI) (43). All study sites obtained approval from local institutional review boards or ethics committees. All participants provided written informed consent.

Imaging Data Preprocessing

Anatomical brain images were preprocessed at Duke University with a standardized neuroimaging and QC pipeline developed by the ENIGMA Consortium (<http://enigma.ini.usc.edu/protocols/imaging-protocols/>) (44). CT and SA measurements were generated by FreeSurfer software (<https://surfer.nmr.mgh.harvard.edu>) based on the Destrieux atlas (45) that contains 74 regions per hemisphere. In brief, white matter surfaces were deformed toward the gray matter boundary at each surface vertex. CT was calculated based on the average distance between the parcellated portions of white and pial surfaces within each region, and SA was measured as the area within each region. The CT and SA estimates for each region and subject were entered into further respective analyses. The quality of structural images per hemisphere from each site (in 21 of 29 sites) was assessed with the Euler number, which is a measure of topological complexity of the reconstructed cortical surface (46). As shown in Supplementary Table S3, the Euler number did not show significant difference between PTSD and non-PTSD groups at most sites except for Duke University (DeBellis) and INTRUST.

Harmonizing Data Across Sites

ComBat was utilized to harmonize CT and SA values by removing the effects of study sites while preserving inherent biological associations in the data (47). *ComBat* achieves harmonization by first modeling expected imaging features as linear combinations of the biological variables and site effects whose error term is further modulated by site-specific scaling factors. Secondly, *ComBat* applies empirical Bayes to improve the estimation of site parameters for small samples. This method effectively removes unwanted sources of site variability thereby increasing the power and reproducibility of subsequent statistical analyses of multi-site studies on CT (48, 49). PTSD diagnosis, age, and sex were designated as biological variables, but PTSD severity and depression diagnosis were not designated as biological variables because they were highly correlated with PTSD diagnosis, and some participants were missing information on PTSD severity and depression.

Adjusting for Confounding Factors

Age, age², sex, and mean whole-brain CT (or SA) estimates were regressed from the CT (or SA) estimates with a linear model (50). The age² term adjusted for possible nonlinear

effects of age on CT (or SA). The mean whole-brain CT (or SA) estimate was included as a regressor to adjust for globally higher CT (or SA) estimates to reflect larger regional CT (or SA) estimates.

All Region SC Analyses

Pearson correlation coefficients were computed across subjects per group between the CT (or SA) estimates for each of the $(148 \times 147) / 2 = 10,878$ pairs of regions. All correlation coefficients were *r*-to-*z* transformed to improve normality and yielded a unique connectivity matrix for each participant group. The resulting matrix quantified the SC, which was interpreted for the present study as a measure of the connectivity strength between regions. The difference in whole-brain SC between PTSD and non-PTSD was calculated for each pair of regions by permuting the group label for subjects 5,000 times (11). False discovery rate (FDR) was thresholded at 5% to correct for 10,878 comparisons between pairs of regions (51).

Top-*n* Regions SC Analyses

The pipeline for the top-*n* regions SC analysis is shown in Fig. 1A. Different from the above-mentioned all-region SC analysis, the top-*n* regions SC analysis was limited to networks consisting of the top-*n* ($n = 2$ to 148) cortical regions that were selected by rank-ordering PTSD-related changes in CT or SA by Cohen's *d* effect sizes (Fig. 2 and Supplementary Tables S4). *Standardized* effect size estimates such as Cohen's *d* are independent of the units or magnitude of CT or SA values. We examined three types of rank-ordering of regions to generate 3 network types (see Fig. 1B): (i) regions with higher CT in PTSD than non-PTSD were ordered from the largest positive to the largest negative effect size were used to construct *hypertrophic* networks, (ii) regions with higher CT in non-PTSD than PTSD were rank-ordered from the largest positive to the largest negative effect size were used to construct *atrophic* networks, and (iii) regions identified by comparing CT in PTSD to non-PTSD groups were rank-ordered from smallest to largest effect size were used to construct *stable* networks. The same approach used for CT was repeated for SA. Thus, for $n=5$, the top-5 regions based on between group differences in effect size were used to form networks, for $n=20$, the top-20 regions based on between group differences in effect size were used to form networks, etc. An illustration depicting CT-based hypertrophic networks for top-3, top-10 and top-50 regions are shown in Fig. 1C.

Actual Networks versus Random Networks

The mean SC (mean of all positive SC values within a network) of an actual network of the top-*n* regions was contrasted (i.e., mathematical subtraction) with the values of mean SC from 5,000 random networks consisting of *n* randomly chosen regions. This test was performed for SC measured in PTSD and non-PTSD groups, as well as between-group difference in SC. The randomly chosen regions were matched to the top-*n* regions for each value of *n*, based on the number of regions in each hemisphere and the mean Euclidean distance between all possible pairs of regions. The Euclidean distance was calculated based on the distance between the centers of cortical regions. This approach was conducted by generating 5,000 randomly chosen sets of *n*-regions that were matched on the number of regions per hemisphere. We then repeatedly replaced the set of *n*-regions with the largest

or smallest mean distance by a randomly generated set of n -regions until the mean distance of the actual regions was not significantly different than the mean distance from the set of randomly chosen n -regions (one-sample t -test thresholded at 5%), or the number of searches exceeded 3,000.

Replication Analyses

To test the reliability of our results comparing actual networks to random networks in the PTSD group, non-PTSD group, and PTSD versus non-PTSD, we conducted 5,000 iterations of leaving out three sites to calculate the 95% confidence interval of mean SC for each type of network. For each iteration, we randomly removed 3 out of 29 sites (~10% of all sites) and performed the same analyses on the remaining data including data harmonization, adjustment for covariates, calculation of the mean SC of the actual network with top- n regions for the PTSD group, non-PTSD group, and the between-group comparison as described above. Our approach is more robust than performing a split sample reproducibility test, which may lead to a false confirmation or a false rejection of results. Removing three sites is superior to removing a single site at each iteration given that some of the sites have relatively small sample sizes, which may also produce spurious results.

PTSD By Sex Interaction

To investigate the modulation of sex on PTSD-related SCNs, we first divided PTSD and non-PTSD groups into male and female subgroups (see Supplementary Table S5). Subsequently, the CT-based (or SA-based) mean SC between the top- n regions within each type of network (atrophic, hypertrophic) was contrasted with CT-based (or SA-based) mean SC from 5,000 randomly chosen sets of n -regions. This test was performed for the SC measured in each of the sub-groups, and for the difference in SC between subgroups. Two-way interactions were calculated by first contrasting PTSD (relative to its random networks) to non-PTSD (relative to its random networks) within each sex subgroup, and then calculating the difference between the two contrasts. More detailed comparisons between each pair of subgroups were conducted when there was a significant interaction effect between PTSD diagnosis and sex.

PTSD By Age Interaction

To investigate the modulation effect of depression on PTSD-related SCNs, we first divided PTSD and non-PTSD groups into eight decadal subgroups based on age: Age<10, 10 Age<15, 15 Age<20, 20 Age<30, 30 Age<40, 40 Age<50, 50 Age<60, Age 60 (see Supplementary Table S6). Subsequently, the CT-based (or SA-based) mean SC between the top- n regions within each type of network was contrasted with the values of CT-based (or SA-based) mean SC from 5,000 randomly chosen sets of n -regions. This test was performed for the SC measured in each of the sub-groups, as well as for the difference in SC between subgroups. Two-way interactions were calculated by first contrasting PTSD (relative to its random networks) to non-PTSD (relative to its random networks) within each age subgroup, and then calculating the difference between the two contrasts. More detailed comparisons between each pair of subgroups were conducted when there was a significant interaction effect between PTSD diagnosis and age.

PTSD X Depression Interaction

To investigate the modulation effect of depression on PTSD-related SCNs, we first divided PTSD and non-PTSD groups into subgroups based on depression diagnosis consisting of two subgroups: depressed and non-depressed (see Supplementary Table S7). Subsequently, the CT-based (or SA-based) mean SC between the top- n regions within each type of network was contrasted with the values of CT-based (or SA-based) mean SC from 5,000 randomly chosen sets of n -regions. This test was performed for the SC measured in each of the sub-groups, as well as for the difference in SC between subgroups. Two-way interactions were calculated by first contrasting PTSD (relative to its random networks) to non-PTSD (relative to its random networks) within each depression subgroup, and then calculating the difference between the two contrasts. More detailed comparisons between each pair of subgroups were conducted when there was a significant interaction effect between PTSD diagnosis and depression.

Global and Individual Tests

We performed two tests of statistical significance that were complementary to each other – the global test and the individual test. The mean SC between n -regions was plotted as a function of n (from $n = 2$ to 148; Fig. 1C). As implemented by Wannan et al. (2019), the area under this curve (AUC) was used to compute the p -value for the global test, which was the proportion of AUC values from the randomly generated networks of n -regions that exceeded or equaled the AUC values for the actual networks of top- n regions. The p -value for the individual test was calculated for each value of n as the proportion of mean SC values from randomly chosen sets of n regions that exceeded or equaled the mean SC from the actual top- n network. The global p -value gives an overall estimate of the connections regardless of network size, while the individual p -value reflects how connections are influenced by the size of cortical networks. Both global and individual p -values were derived from two-tailed tests.

Corrections for Multiple Comparisons

The Bonferroni method was employed to correct for the number of comparisons, i.e., 2 (CT-based and SA-based networks) by 3 (atrophic, hypertrophic, and stable networks), in global tests and individual tests. This method was also employed to correct for the 6 comparisons (i.e., all pairs among 4 subgroups) where there was a significant interaction between PTSD diagnosis and depression, or sex, or age. The FDR method (51) was further employed in individual tests to correct for network size (totally 147, $n = 2$ to 148). All p -values shown are corrected for multiple comparisons.

Correlations Between Regional Average SC and Effect Size of Cortical Changes

To examine whether brain hubs that are strongly connected with other areas (52), played a role in the spatial distribution of PTSD-related cortical changes, we investigated the association between the effect size of cortical changes for each region and the average of positive SC between said region and all the other cortical regions. This association was calculated by Pearson's correlation across regions separately in CT-based and SA-based networks in PTSD and non-PTSD groups.

Results

Methodologic Confirmation of Rank Ordering

Actual versus Random Networks in PTSD.—As displayed in Fig. 3 and Table 2, global tests showed that PTSD patients had higher mean SC in CT-based ($p < 0.001$) and SA-based ($p = 0.017$) atrophic networks, CT-based ($p = 0.029$) and SA-based ($p = 0.017$) hypertrophic networks, and CT-based ($p < 0.001$), but not SA-based ($p > 0.5$) stable networks when compared to the corresponding random networks. No individual test results survived correction ($p\text{-values} > 0.05$). The results of this analysis serve as methodologic confirmation for selecting regions, which are rank-ordered by effect size, in forming SCNs of interest. The analysis of stable networks highlights this point most clearly. Although the stable regions individually differ the least between groups, the networks they form differ significantly in SC between group, except for SA-based stable SCNs.

Actual versus Random Networks in non-PTSD.—As displayed in Fig. 4 and Table 2, global tests showed that the non-PTSD participants had higher mean SC in CT-based ($p < 0.001$) and SA-based ($p < 0.001$) atrophic networks, in SA-based ($p = 0.014$), but not CT-based ($p = 0.139$) hypertrophic networks, and neither CT-based ($p = 0.264$) nor SA-based ($p = 0.732$) stable networks when compared to the corresponding random networks. Individual tests showed that the non-PTSD participants had higher mean SC in CT-based atrophic networks consisting of the top-69, 82, and 93 regions ($p\text{-values} < 0.05$), compared to the corresponding random networks. No other individual test results survived correction ($p\text{-values} > 0.05$). The results of this analysis serve as methodologic confirmation for selecting regions, which are rank-ordered by effect size, in the formation of *atrophic* SCNs of interest. Methodologic confirmation was achieved for SA-based hypertrophic SCNs, but not for CT-based hypertrophic SCNs. Methodologic confirmation for stable SCNs was not achieved in the non-PTSD group.

Effect Size of CT and SA differences

Effect sizes for between-group differences in CT and SA are shown in Fig. 2 and reported in Supplementary Tables S4. Effect sizes ranged from -0.103 (atrophic) to $+0.112$ (hypertrophic) for CT, and from -0.110 (atrophic) to $+0.083$ (hypertrophic) for SA.

SC within Top-n Regions

PTSD versus Non-PTSD.—As displayed in Fig. 5 and Table 2, global tests showed that PTSD versus non-PTSD participants had lower mean SC in both CT-based ($p = 0.014$) and SA-based ($p = 0.024$) atrophic networks. As shown in Supplementary Tables S4, the top-15 regions in the CT-based atrophic network included R-superior temporal gyrus, R inferior insula, R parahippocampal gyrus, L superior temporal gyrus, L long insular gyrus and central sulcus, L occipital middle gyrus, R middle occipital sulcus, R anterior occipital sulcus, L inferior insula, L occipital inferior sulcus and gyrus, R supramarginal gyrus, R insular gyrus and central sulcus, L gyrus rectus.

The top-15 regions in the SA-based atrophic network included L H-shaped orbital sulcus, R inferior insula, R orbital sulcus, R central sulcus, L marginal cingulate sulcus, L subcallosal

gyrus, L inferior insula, L medial orbital sulcus, R anterior cingulate gyrus, R medial orbital sulcus, L superior and transverse occipital sulcus, R sulcus intermedius primus (Jensen), L precentral sulcus, fronto-marginal gyrus, L lateral superior temporal gyrus.

No significant differences in CT-based ($p = 0.098$) and SA-based ($p > 0.5$) hypertrophic networks, as well as CT-based ($p > 0.5$) and SA-based ($p > 0.5$) stable networks. No individual test results survived correction (p -values > 0.05).

Replication Analyses Results.—As shown in Fig. 6, the global-tests results displayed in Figs 3, 4, 5 and Table 2 are reliable because the AUC of mean SC for the results based on all 29 sites were always located within the 95% confidence interval of the AUC of mean SC from 5,000 iterations leaving out 3 different sites with each iteration of the analysis across all types of networks.

Only a very small number of the individual-tests results were beyond their 95% confidence intervals. They are the CT-based stable network with top-24 regions in the non-PTSD group, the SA-based atrophic network with top-11 regions for the PTSD versus non-PTSD comparison, and the SA-based hypertrophic networks with top-32, 33, 34, or 35 regions for the PTSD versus non-PTSD comparison.

Interaction Effects

PTSD x Depression Interaction.—As listed in Fig. 7, global tests showed a significant interaction effect in CT-based atrophic networks ($p = 0.029$; Fig. 7A). Further analyses showed that participants with depression alone had greater mean SC than the participants with PTSD and comorbid depression ($p < 0.001$), PTSD alone ($p < 0.001$), and healthy controls ($p < 0.001$).

There was a significant interaction effect in SA-based atrophic networks ($p = 0.001$; Fig. 7B). Further analyses showed that participants with PTSD alone had greater mean SC than participants with PTSD and comorbid depression ($p < 0.001$) and healthy controls ($p = 0.014$). Participants with depression alone also had greater mean SC than participants with PTSD and comorbid depression ($p < 0.001$) and healthy controls ($p < 0.001$).

There was a significant interaction effect in SA-based hypertrophic networks ($p = 0.014$; Fig. 7D). Further analyses showed that PTSD patients with co-morbid depression ($p = 0.029$) and healthy controls ($p < 0.001$) had greater mean SC than those with depression alone. No other global tests (p -values > 0.2) and no individual tests (p -values > 0.05) survived correction.

Effects of PTSD x Sex interaction.—Global tests showed that females with PTSD ($p = 0.029$) and males without PTSD ($p = 0.014$) had greater mean SC in CT-based atrophic networks than females without PTSD. Males without PTSD had greater mean SC in CT-based stable networks than males with PTSD ($p = 0.014$) and females without PTSD ($p < 0.001$). No significant PTSD x sex interaction effect (global p -values > 0.1) was found in the other types of networks.

Effects of PTSD x Age interaction.—An inverted-U relationship between decadal age and mean SC was observed in CT-based atrophic networks in both non-PTSD participants, peaking in the 3rd decade, and PTSD patients, peaking in the 2nd decade, and SA-based hypertrophic networks in PTSD patients and non-PTSD patients, both peaking in the 2nd decade. PTSD-related differences in mean SC were observed in different age groups, especially in the 1st decade, represented by lower mean SC in CT-based atrophic networks ($p < 0.001$) and SA-based hypertrophic networks ($p = 0.019$), as well as higher mean SC in CT-based hypertrophic ($p < 0.001$) and stable ($p < 0.001$) networks, in patients with PTSD compared to non-PTSD participants.

Correlations between Regional Average SC and Effect Size of Cortical Changes

No significant correlation was found in CT-based ($R = -0.091$, $p = 0.270$) and SA-based ($R = 0.021$, $p = 0.795$) networks of patients with PTSD. No significant correlation was found in CT-based ($R = -0.110$, $p = 0.183$) and SA-based ($R = -0.003$, $p = 0.967$) networks of non-PTSD participants. These negative results suggest that the spatial distribution of PTSD-related cortical changes are not related to the brain hubs that are strongly connected to other areas (reflected by high SC between said region and all the other cortical regions), but are associated with the strength of connections among regions.

Discussion

We investigated the mean structural covariance of CT-based and SA-based networks composed of regions with the most atrophic, most hypertrophic, and most stable relationships to PTSD relative to trauma-exposed controls. Three network classes were composed of regions selected based on the effect size of PTSD-related differences in regional CT and SA. We compared the mean SC of these networks to random networks in PTSD and non-PTSD groups, respectively. We also investigated the role of PTSD diagnosis and PTSD severity on SC, and interaction effects of PTSD with age, sex and depression. We performed methodologic confirmation by demonstrating that PTSD and non-PTSD groups had higher SC in CT-based atrophic networks, SA-based atrophic networks, and SA-based hypertrophic networks than corresponding random networks (Table 2 and Fig. 3, 4). Methodologic confirmation also showed the PTSD group had higher SC in CT-based hypertrophic networks and CT-based stable networks than corresponding random networks. Of particular interest and consistent with *a priori* hypotheses, we discovered that participants with PTSD had lower SC than trauma-exposed non-PTSD participants in CT-based and SA-based atrophic networks (Table 2 and Fig. 5). Furthermore, depression alone had higher SC in both CT- and SA-based atrophic networks, and lower SC in SA-based hypertrophic networks compared to PTSD with comorbid depression and compared to healthy controls (Fig. 7A, B, D). Patients with PTSD alone showed lower SC in CT-based atrophic networks than patients with depression alone (Fig. 7A), and higher SC in SA-based atrophic networks compared to PTSD with comorbid depression and to healthy controls (Fig. 7B).

Our main finding shows that the networks composed of regions having the greatest PTSD-related atrophy, have significantly lower network covariance in the PTSD group than in the trauma-exposed control group. This finding was present for networks derived from both CT

and SA. A number of interpretations of this finding are tenable. First, we note a degree of consistency between CT-based and SA-based networks in our results concerned with PTSD diagnosis. Many cortical regions within networks that are affected by PTSD are strongly implicated (by definition) in PTSD such as insula, orbital frontal cortex, anterior cingulate, and subcallosal gyrus. However, our present study is not focused on the status of individual regions, but rather, in network perturbations associated with PTSD. Of particular note, the functional networks previously implicated in PTSD comport with the present structural network findings such as in low-level perceptual networks (53), salience network (54), default mode network (55), and central executive network (56), also referred to as the fronto-parietal network (57). Our finding of structural networks involving medial prefrontal cortex, posterior cingulate cortex (SA-based only), and angular gyrus, are canonical regions of the default mode network, which is also strongly implicated in PTSD. Our finding of structural networks involving anterior cingulate cortex, and insular cortex recapitulated salience network differences that have been reported in PTSD. However, our structural network findings did not recapitulate prior reports of central executive network involvement in PTSD, but the largest meta-analysis of network differences in PTSD did not find central executive network involvement (54), either. Unfortunately, there is a profound dearth of published findings on structural covariance network differences in PTSD for purposes of comparison. It is possible that the cortical networks or network mechanisms that propagate PTSD-related structural atrophy are dampened by the disease itself or dampened unevenly across brain topography. Alternatively, individuals with weaker connections in atrophic networks may be more vulnerable to PTSD. Unfortunately, our cross-sectional study design is unable to discern causal factors that contribute to PTSD.

It is worth noting, the same areas may serve as the top regions in different types of networks, suggesting their essential and diverse roles in cortical connections. For instance, the right inferior segment of the circular sulcus of the insula is a top-2 region within the CT- and SA-based atrophic networks. The top-2 regions were distributed across networks included orbitofrontal, lateral prefrontal, insular, superior temporal, and inferior temporal cortices (see Supplementary Table S4). Hyperactivity in the insula and inferior frontal areas, widely reported in PTSD (58)(58)(56)(58)(58)(58), reflects enhanced detection of, and response to, internal and external threat stimuli (59). Larger volumes in inferior frontal gyrus and precentral gyrus relate to an increased number of intrusive memories (60), which is a prominent and distressing symptom of PTSD. The orbitofrontal cortex is involved in extinction memory processes (61) that play a central role in the etiology and maintenance of PTSD (62). Reduced grey matter volume (63) and lower SC nodal centrality in the orbitofrontal cortex (64) are evident in maltreated youth with PTSD compared to youth without PTSD. The regions mentioned are strongly implicated in PTSD, not just as isolated regions, but also within the context of their structural network topography. The functions of these regions may be incorporated into and modulated by networks containing different nodes and with diverse network sizes.

In addition to functional networks, converging evidence of inflammatory processes, which contribute to PTSD, preferentially impact the same regions that constitute atrophic networks we identified. The medial prefrontal cortex, insula, and anterior cingulate are all preferentially impacted by inflammatory processes that plague PTSD and other fear-

and anxiety-based conditions (65). While the amygdala and hippocampus are also affected by inflammatory processes, we included only cortical structures, which have a uniquely measurable CT and SA. Stress hormones pose pronounced deleterious effects to the medial prefrontal cortex (66) and to the orbitofrontal cortex (67), which also featured prominently in the atrophic networks we linked to PTSD. Evidence of stress hormone effects on the brain are strongly informed by animal models. In humans, frontoparietal connectivity is disrupted after exposure to one month of intense academic stress (68). Thus, stress induced changes to medial prefrontal cortex, orbital frontal cortex, and frontoparietal regions were present in atrophic networks we linked to PTSD. Epigenetic effects on the brain have been linked to intergenerational trauma and its effects, particularly on the medial prefrontal cortex (69, 70). Epigenetic regulation of the FKBP5 gene in response to early trauma is implicated in PTSD pathogenesis (71). The methylation of FKBP5 CpG1 of intron 7 is associated with lower gray matter in bilateral orbital frontal gyrus (72). Epigenetic regulation at the stress-responsive genes that encode the pituitary adenylate cyclase-activating polypeptide (ADCYAP1) and CpG island methylation levels of its receptor ADCYAP1R1 predict PTSD symptom severity (71). Thus, inflammation, stress hormones and epigenetics, all appear to play a role in SC network difference linked to PTSD.

CT-based network SC reflects the integrity of white matter fiber bundles represented by inter-regional connections (8). This relationship may reflect that factors influencing cortical remodeling are transported from one region to another via a white matter conduit that supports trans-neuronal or trans-synaptic communication (73, 74), and produces contemporaneous CT changes throughout the network. It is possible that dynamic processes in white matter fiber tracts influence neural signaling or trophic support between structurally connected brain regions and induce postsynaptic dendritic covariation and concomitant CT change (75). Similar mechanisms may apply to SA-based networks although there are fewer corroborating reports (76). Across participants from both groups, we observed higher mean SC in both CT-based and SA-based atrophic, and SA-based hypertrophic networks as compared to random networks. These findings show that inter-regional connections effect cortical remodeling regardless of diagnostic status, as well as CT- and SA-based network covariance in PTSD. Whereas there is little evidence of white matter differences in adult trauma induced PTSD, child trauma induced PTSD (77) shows compromise of white matter connectivity. This disruption may invoke loss of healthy neuronal signaling or a retreat of trophic support needed by vulnerable regions, and eventually to postsynaptic dendritic retraction and atrophy (78). Mechanisms that support the propagation of PTSD-associated cortical variation, its relationship to white matter structure, its relationship to functional connectivity, and the role of trans-synaptic or trans-neuronal spread, will require the application of multi-modal imaging methods.

The present study extends several facets of earlier SC reports in PTSD. Broadly, the present study has three major methodological differences compared to published reports: **(i)** While we focused only on regions at the extremes of between-group differences in constructing networks, prior studies have considered all regions in such covariance networks, which compromises power compared to the feature reduction strategy we implemented. **(ii)** Our sample size (n=3,400) is 10-fold larger than any previous study (n=317) (11). **(iii)** Two prior

studies were focused on children and adolescents ($n=88$ and $n=120$) (12, 64) and a third study focused on remitted PTSD in adults ($n=317$) (11). Thus, the present study is uniquely situated with respect to statistical power, a target population from a broad age-range, and illness chronicity. Our study extends the methodology developed by Wannan et al., (26) by investigating CT and SA of hypertrophic, atrophic, and stable networks separately rather than considering only the CT of atrophic networks. We show that some brain networks, independent of disease, mirror the spatial distribution of disease-related changes in cortical morphometry, thus confirming the work of Wannan et al. (26). Our results demonstrate for the first time that the SC of three different network classes are each uniquely associated with PTSD. We explicitly investigated *stable networks*, which could be summarily dismissed as negative findings since the contributing regions have minimal between-group differences. However, negative findings do not necessarily indicate that group differences in SC are absent. Negative findings may indicate insufficient statistical power. The sample size of the present study provides sufficient power to detect extremely small effect sizes, which we may confidently interpret as negative findings that reflect networks of *stable* regions.

It is important to contrast the interpretation of CT- with SA-based networks. The relationship between CT and SA is complex involving myriad factors including brain hemisphere, brain region, age, IQ, disease, genetics, and many other factors (33, 79). The large size of the human cortex, in comparison to other animals, is driven primarily by expansion of SA, not an increased CT (80), and achieved through gyral folding. Individual differences in cortical volume are largely attributable to variability in surface area as opposed to cortical thickness (81). While CT and SA are highly heritable ($r_g = 0.81$ and 0.89 , respectively), the genetic correlation between CT and SA is exceedingly low ($r_g = 0.08$). The influence of environment on CT and SA is also relatively low, accounting for 20% of their variance (82). Findings from structural MRI of 51,665 genotyped individuals show that common genetic variants explain greater phenotypic variance in SA (8 to 31%) than in CT (1 to 13%). Strikingly, 175 unique genetic loci were associated with SA, but only 10 unique loci were associated with CT (83). Understanding the functional roles of these genetic loci will contribute to interpretation of CT-based and SA-based structural connectivity, which will help us to understand the genetic contribution of remodeling of cortical topography in PTSD. Perhaps identifying common genetic variants that explain CT- and SA- based structural connectivity between regions and within networks will provide insights into the genetic architecture of the structural connectome (10).

Patients with depression alone showed higher mean SC in both CT-based and SA-based atrophic networks, and lower mean SC in SA-based hypertrophic networks, as compared to healthy controls. These results suggest that depression is associated with more coordinated propagation of CT and SA reductions, and less coordinated SA increases. Our result is consistent with previous reports that depression is associated with widely distributed CT reductions (84). Patients with PTSD alone showed lower mean SC in CT-based atrophic networks than patients with depression alone, suggesting that PTSD is associated with more coordinated decline throughout CT-based networks than depression. We also found that PTSD with comorbid depression was associated with lower mean SC in CT-based atrophic networks than depression alone, lower mean SC in SA-based atrophic networks compared to PTSD alone and depression alone, and higher mean SC in SA-based hypertrophic networks

relative to depression alone. Previous studies have documented greater volume reductions in cortical structures including anterior/middle cingulate cortex, orbitofrontal cortex, and dorsolateral prefrontal cortex in PTSD with comorbid depression that are absent in either disorder alone (85). Behaviorally, higher levels of distress (86), impaired neurocognitive function (87), and greater risk for suicide (88) are present in comorbid PTSD and depression compared to PTSD alone. PTSD with comorbid depression, relative to either disorder alone, may be associated with larger disruptions of individual cortical regions and their network SC, which may explain greater symptom severity.

The cortical regions showing high SC with other regions may represent hubs in brain-network topology (52). Indeed, we reported previously that PTSD is accompanied by altered CT estimates as well as differences in nodal centrality in some brain hubs (12), which is also supported by an earlier study by Mueller, Ng (3). However, we did not find a significant relationship between the effect size of PTSD-related CT (or SA) change in any given region and its average connections with all the other regions. Our findings suggest that PTSD-related cortical changes are shaped by brain networks with strong covariance, rather than hubs that are highly connected to other regions.

We explored the modulation of PTSD-related differences in SCN by sex and age, and modulation of SCNs by PTSD symptom severity. We found that (Supplementary Fig. S1), females with PTSD and males without PTSD had greater SC in CT-based atrophic networks than females without PTSD. Males without PTSD had greater mean SC in CT-based stable networks than males with PTSD and females without PTSD. Diffusion-based structural connectome studies in youth show that males have stronger connections between regions for perception and coordinated action, whereas females have stronger connections between analytical and intuitive processing modes (89), demonstrating the sex-related differences in brain connections. We also found (Supplementary Fig. S2) an inverted U-shaped relationship between age and SC in CT-based atrophic networks that peaked at 20–30 years in non-PTSD and 15–20 years in PTSD, whereas SA-based hypertrophic networks peaked at 10–15 years in both groups. We found significant PTSD-related SC differences in some age groups, particularly < 10 years, as demonstrated by higher SC in CT-based hypertrophic and stable networks, lower SC in CT-based atrophic networks, and lower SC in SA-based hypertrophic networks. Our results suggest that multiple networks undergo transformation in a coordinated fashion to support the development of the brain as well as PTSD symptoms, particularly during early childhood. A previous longitudinal study in healthy young people (9) showed that similar global and nodal topological properties as well as mesoscopic features are shared by SC networks and maturation networks, which are based on each region's slope of maturation with age and pairwise correlations in the rate of maturation across subjects.

Strengths and Limitations

A major strength of our study is a large cohort of over 3,400 participants that represent diverse geography, demography (sex, age, race), trauma type (military, sexual violence, natural disasters) and clinical comorbidity. This sample heterogeneity enhances the generalizability and reproducibility of our findings. Harmonization of CT and SA measures

sourced from 29 international sites with different MRI scanners was addressed with *ComBat* (47). A major strength our methodology is empirical confirmation that the most atrophic regions, or most hypertrophic regions, constitute the networks with the greatest change in SC. The possibility that SC might be most affected by PTSD in networks formed of random regions, i.e. where PTSD associated changes of individual regions are completely unremarkable, has been robustly addressed.

The following limitations warrant consideration when interpreting the present results. Firstly, our study is based on cross-sectional data which lacks longitudinal information to inform neurodevelopmental processes. Combining neuroimaging data from multiple longitudinal scans on each subject over several years of follow-up, preferably with pre-trauma and post-trauma observations, may help us to better understand the developmental changes in SC networks among trauma-exposed and PTSD subjects. Secondly, image quality reflected by the Euler number was not significantly different between PTSD and non-PTSD groups in most sites except for Duke University (DeBellis) and INTRUST. Higher image quality is associated with greater CT in dorsolateral prefrontal cortex, superior parietal cortex, and lateral temporal cortex, as well as smaller CT in occipital and posterior cingulate cortex (46). Cortical morphometry and therefore SC may be biased by the PTSD-related differences in image quality at two sites. However, our leave-three-sites-out analyses indicated that our results are reliable. Future studies on cortical morphometry and cortico-cortical SCNs should consider including the image quality as a covariate in statistical models. Finally, information on illness chronicity, developmental timing of trauma, childhood maltreatment, and other comorbidities such as anxiety, were unavailable in the datasets shared with us by our Consortium partners. Future research comparing trauma-exposed individuals without PTSD to trauma-unexposed individuals could offer evidence supporting a hypothetical *resilience network*. Similarly, differences in patients with remitted PTSD compared to chronic PTSD could support the existence of a hypothetical *recovery network*. Future research could also compare patient groups exhibiting specific symptom clusters of PTSD.

Conclusions

Cortico-cortical connections shape the topography of PTSD-related differences in cortical morphometry. Thus, regional cortical morphometry associated with PTSD, does not occur in isolated brain regions and independent of differences seen in other cortical regions. Rather, the regions whose morphometry are most affected by PTSD, albeit not significantly, form networks whose covariance structure is significantly affected by PTSD diagnosis and symptom severity. This finding fundamentally and significantly extends our understanding about the effects of PTSD on brain structure. Namely, cortical regions must be viewed from a wholistic standpoint as acting within the context of networks that are affected in coordinated manner by PTSD and further modulated by comorbid depression, sex, and age. The structural covariance networks that are perturbed in PTSD comport with converging evidence from resting state functional connectivity networks and networks impacted by stress hormones, inflammation, and epigenetics.

Supplementary Material

Refer to Web version on PubMed Central for supplementary material.

Authors

Delin Sun^{1,2}, Gopalkumar Rakesh^{1,2}, Emily K. Clarke-Rubright^{1,2}, Courtney C. Haswell^{1,2}, Mark Logue^{3,4,5,6}, Brian M. O'Leary⁷, Andrew S. Cotton⁷, Hong Xie⁷, Emily L. Dennis^{8,9,10,11}, Neda Jahanshad⁹, Lauren E. Salminen⁹, Sophia I. Thomopoulos⁹, Faisal Rashid⁹, Christopher R. K. Ching⁹, Saskia B. J. Koch^{12,13}, Jessie L. Frijling¹², Laura Nawijn^{12,14}, Mirjam van Zuiden¹², Xi Zhu^{15,16}, Benjamin Suarez-Jimenez^{15,16}, Anika Sierk¹⁷, Henrik Walter¹⁷, Antje Manthey¹⁷, Jennifer S. Stevens¹⁸, Negar Fani¹⁸, Sanne J.H. van Rooij¹⁸, Murray Stein¹⁹, Jessica Bomyea¹⁹, Inga Koerte^{8,20}, Kyle Choi²¹, Steven J.A. van de Werff^{22,23}, Robert R. J. M. Vermeiren²², Julia Herzog²⁴, Lauren A.M. Lebois^{25,26}, Justin T. Baker²⁷, Kerry J. Ressler^{18,25,26}, Elizabeth A. Olson^{25,28}, Thomas Straube²⁹, Mayuresh S. Korgaonkar³⁰, Elpiniki Andrew³¹, Ye Zhu^{32,33}, Gen Li^{32,33}, Jonathan Ipser³⁴, Anna Hudson³⁵, Matthew Peverill³⁶, Kelly Sambrook³⁷, Evan Gordon^{38,39,40}, Lee Baugh^{41,42,43}, Gina Forster^{41,42,44}, Raluca Simons^{42,45}, Jeffrey Simons^{43,45}, Vincent Magnotta⁴⁶, Adi Maron-Katz⁴⁷, Stefan du Plessis⁴⁸, Seth Disner^{49,50}, Nicholas Davenport^{49,50}, Dan Grupe⁵¹, Jack Nitschke⁵², Terri A. deRoos-Cassini⁵³, Jacklynn Fitzgerald⁵⁴, John H. Krystal^{55,56}, Ifat Levy^{55,56}, Miranda Olf^{12,57}, Dick J. Veltman⁵⁸, Li Wang^{32,33}, Yuval Neria^{15,16}, Michael D. De Bellis⁵⁹, Tanja Jovanovic^{18,60}, Judith K. Daniels⁶¹, Martha Shenton^{8,62}, Nic J.A. van de Wee^{22,23}, Christian Schmahl²⁴, Milissa L. Kaufman^{25,63}, Isabelle M. Rosso^{25,28}, Scott R. Sponheim^{49,50}, David Bernd Hofmann²⁹, Richard A. Bryant⁶⁴, Kelene A. Fercho^{41,42,43,65}, Dan J. Stein³⁴, Sven C. Mueller^{35,66}, Luan Phan^{67,68}, Katie A. McLaughlin⁶⁹, Richard J. Davidson^{51,52,70}, Christine Larson⁷¹, Geoffrey May^{38,39,40,72}, Steven M. Nelson^{38,39,40,72}, Chadi G. Abdallah^{55,56}, Hassaan Gomaa⁷³, Amit Etkin^{47,74}, Soraya Seedat⁴⁸, Ilan Harpaz-Rotem^{55,56}, Israel Liberzon⁷⁵, Xin Wang⁷, Paul M. Thompson⁹, Rajendra A. Morey^{1,2,*}

Affiliations

¹Brain Imaging and Analysis Center, Duke University, Durham, NC, USA.

²Department of Veteran Affairs (VA) Mid-Atlantic Mental Illness Research, Education and Clinical Center, Durham, NC, USA.

³National Center for PTSD, VA Boston Healthcare System, Boston, MA, USA.

⁴Department of Psychiatry, Boston University School of Medicine, Boston, MA, USA.

⁵Biomedical Genetics, Boston University School of Medicine, Boston, MA, USA.

⁶Department of Biostatistics, Boston University School of Public Health, Boston, MA, USA.

⁷Department of Psychiatry, University of Toledo, Toledo, OH, USA.

⁸Psychiatry Neuroimaging Laboratory, Brigham & Women's Hospital, Boston, MA, USA.

⁹Imaging Genetics Center, Stevens Neuroimaging & Informatics Institute, Keck School of Medicine of USC, Marina del Rey, CA, USA.

¹⁰Department of Neurology, University of Utah, Salt Lake City, UT, USA.

¹¹Stanford Neurodevelopment, Affect, and Psychopathology Laboratory, Stanford, CA, USA.

¹²Department of Psychiatry, Amsterdam University Medical Centers, Academic Medical Center, University of Amsterdam, Amsterdam, The Netherlands.

¹³Donders Institute for Brain, Cognition and Behavior, Centre for Cognitive Neuroimaging, Radboud University Nijmegen, Nijmegen, The Netherlands.

¹⁴Department of Psychiatry, Amsterdam University Medical Centers, VU University Medical Center, VU University, Amsterdam, The Netherlands.

¹⁵Department of Psychiatry, Columbia University Medical Center, New York, NY, USA.

¹⁶New York State Psychiatric Institute, New York, NY, USA.

¹⁷University Medical Centre Charité, Berlin, Germany.

¹⁸Department of Psychiatry and Behavioral Sciences, Emory University School of Medicine, Atlanta, GA, USA.

¹⁹Department of Psychiatry, University of California San Diego, La Jolla, CA, USA.

²⁰Department of Child and Adolescent Psychiatry, Psychosomatics, and Psychotherapy, Ludwig-Maximilians-Universität, Munich, Germany

²¹Health Services Research Center, University of California, San Diego, La Jolla, CA, USA

²²Department of Psychiatry, Leiden University Medical Center, Leiden, The Netherlands.

²³Leiden Institute for Brain and Cognition, Leiden, The Netherlands.

²⁴Department of Psychosomatic Medicine and Psychotherapy, Central Institute of Mental Health, Medical Faculty Mannheim, Heidelberg University, Heidelberg, Germany.

²⁵Department of Psychiatry, Harvard Medical School, Boston, MA, USA.

²⁶Division of Depression and Anxiety Disorders, McLean Hospital, Belmont, MA, USA.

²⁷Institute for Technology in Psychiatry, McLean Hospital, Harvard University, Belmont, MA, USA.

- ²⁸Center for Depression, Anxiety, and Stress Research, McLean Hospital, Belmont, MA, USA.
- ²⁹Institute of Medical Psychology and Systems Neuroscience, University of Münster, Münster, Germany.
- ³⁰Brain Dynamics Centre, Westmead Institute of Medical Research, University of Sydney, Westmead, NSW, Australia.
- ³¹Department of Psychology, University of Sydney, Westmead, NSW, Australia.
- ³²Laboratory for Traumatic Stress Studies, Chinese Academy of Sciences Key Laboratory of Mental Health, Institute of Psychology, Chinese Academy of Sciences, Beijing, China.
- ³³Department of Psychology, University of Chinese Academy of Sciences, Beijing, China.
- ³⁴SA MRC Unit on Risk & Resilience in Mental Disorders, Department of Psychiatry and Neuroscience Institute, University of Cape Town, Cape Town, South Africa.
- ³⁵Department of Experimental Clinical and Health Psychology, Ghent University, Ghent, Belgium.
- ³⁶Department of Psychology, University of Washington, Seattle, WA, USA.
- ³⁷Department of Radiology, University of Washington, Seattle, WA, USA.
- ³⁸Veterans Integrated Service Network-17 Center of Excellence for Research on Returning War Veterans, Waco, TX, USA.
- ³⁹Department of Psychology and Neuroscience, Baylor University, Waco, TX, USA.
- ⁴⁰Center for Vital Longevity, School of Behavioral and Brain Sciences, University of Texas at Dallas, Dallas, TX, USA.
- ⁴¹Division of Basic Biomedical Sciences, Sanford School of Medicine, University of South Dakota, Vermillion, SD, USA.
- ⁴²Center for Brain and Behavior Research, University of South Dakota, Vermillion, SD, USA.
- ⁴³Sioux Falls VA Health Care System, Sioux Falls, SD, USA.
- ⁴⁴Brain Health Research Centre, Department of Anatomy, University of Otago, Dunedin, New Zealand.
- ⁴⁵Department of Psychology, University of South Dakota, Vermillion, SD, USA.
- ⁴⁶Department of Radiology, Psychiatry, and Biomedical Engineering, University of Iowa, Iowa City, IA, USA.
- ⁴⁷Department of Psychiatry and Behavioral Sciences, Stanford University, Stanford, CA, USA.
- ⁴⁸Department of Psychiatry, Stellenbosch University, Cape Town, South Africa.

- ⁴⁹Minneapolis VA Health Care System, Minneapolis, MN, USA.
- ⁵⁰Department of Psychiatry, University of Minnesota, Minneapolis, MN, USA.
- ⁵¹Center for Healthy Minds, University of Wisconsin-Madison, Madison, WI, USA.
- ⁵²Department of Psychiatry, University of Wisconsin-Madison, Madison, WI, USA.
- ⁵³Department of Surgery, Division of Trauma and Acute Care Surgery, Medical College of Wisconsin, Milwaukee, WI, USA.
- ⁵⁴Department of Psychology, Marquette University, Milwaukee, WI, USA.
- ⁵⁵Division of Clinical Neuroscience, National Center for PTSD, West Haven, CT, USA.
- ⁵⁶Department of Psychiatry, Yale University School of Medicine, New Haven, CT, USA.
- ⁵⁷ARQ National Psychotrauma Centre, Diemen, The Netherlands.
- ⁵⁸Department of Psychiatry, Amsterdam University Medical Centers, Amsterdam, The Netherlands.
- ⁵⁹Healthy Childhood Brain Development Developmental Traumatology Research Program, Department of Psychiatry and Behavioral Sciences, Duke University, Durham, NC, USA.
- ⁶⁰Department of Psychiatry and Behavioral Neuroscience, Wayne State University School of Medicine, Detroit, MI, USA.
- ⁶¹Department of Clinical Psychology, University of Groningen, Groningen, The Netherlands.
- ⁶²VA Boston Healthcare System, Brockton Division, Brockton, MA, USA.
- ⁶³Division of Women's Mental Health, McLean Hospital, Belmont, MA, USA.
- ⁶⁴School of Psychology, University of New South Wales, Sydney, NSW, Australia.
- ⁶⁵Civil Aerospace Medical Institute, US Federal Aviation Administration, Oklahoma City, OK, USA
- ⁶⁶Department of Personality, Psychological Assessment and Treatment, University of Deusto, Bilbao, Spain.
- ⁶⁷Department of Psychiatry, University of Illinois at Chicago, Chicago, IL, USA.
- ⁶⁸Mental Health Service Line, Jesse Brown VA Chicago Health Care System, Chicago, IL, USA.
- ⁶⁹Department of Psychology, Harvard University, Cambridge, MA, USA.
- ⁷⁰Department of Psychology, University of Wisconsin-Madison, Madison, WI, USA.
- ⁷¹Department of Psychology, University of Wisconsin-Milwaukee, Milwaukee, WI, USA.

⁷²Department of Psychiatry and Behavioral Science, Texas A&M University Health Science Center, Bryan, TX, USA.

⁷³Department of Psychiatry, Pennsylvania State University, State College, PA, USA.

⁷⁴VA Palo Alto Health Care System, Palo Alto, CA, USA.

⁷⁵Department of Psychiatry, University of Michigan, Ann Arbor, MI, USA.

Acknowledgments

DoD W81XWH-10-1-0925; Center for Brain and Behavior Research Pilot Grant; South Dakota Governor's Research Center Grant; CX001600 VA CDA; NIMRC Program Grant #1073041; R01 MH111671; VISN6 MIRECC; German Research Foundation grant to J. K. Daniels (DA 1222/4-1 and WA 1539/8-2); VA RR&D 1K2RX000709; NIMH R01-MH043454; NIMH T32-MH018931; 5U01AA021681-08; K24MH71434; K24 DA028773; R01 MH63407; R01 AA12479; R01 MH61744; K99NS096116; VA RR&D 1K1RX002325; VA RR&D 1K2RX002922; MH101380; ZonMw, the Netherlands organization for Health Research and Development grant to Miranda Olf (40-00812-98-10041); Academic Medical Center Research Council grant to Miranda Olf (110614); VA CSR&D 1K2CX001680; VISN17 Center of Excellence pilot funding; NIMH R01MH105535; NIMH 1R21MH102634; German Federal Ministry of Education and Research (BMBF RELEASE 01KR1303A); German Research Society (Deutsche Forschungsgemeinschaft, DFG; SFB/TRR 58: C06, C07); R01MH111671; R01MH117601; R01AG059874; MJFF 14848; MH098212; MH071537; M01RR00039; UL1TR000454; HD071982; HD085850; R21MH112956; Anonymous Women's Health Fund; Kasparian Fund; Trauma Scholars Fund; Barlow Family Fund; W81XWH-08-2-0159; Department of Veterans Affairs via support for the National Center for PTSD; NIAAA via its support for (P50) Center for the Translational Neuroscience of Alcohol; NCATS via its support of (CTSA) Yale Center for Clinical Investigation; NIH R01 MH106574; F32MH109274; NIMH 1R21MH102634; R01MH113574; R01-MH103291; BOF 2-4 year project to Sven C. Mueller (01J05415); R01MH105355; Dana Foundation (to Dr. Nitschke); the University of Wisconsin Institute for Clinical and Translational Research; a National Science Foundation Graduate Research Fellowship (to Dr. Grupe); the National Institute of Mental Health (NIMH) R01 MH63407 (to De Bellis), R01 AA12479 (to De Bellis), and R01 MH61744 (to De Bellis); R01-MH043454 and T32-MH018931 (to Dr. Davidson); core grant to the Waisman Center from the National Institute of Child Health and Human Development (P30-HD003352); NIMH K23MH112873; Veterans Affairs Merit Review Program (10/01/08 - 09/30/13); L30 MH114379; German Federal Ministry of Education and Research (BMBF RELEASE 01KR1303A); South African Medical Research Council "SHARED ROOTS" Flagship Project; Grant MRC-RFA-FSP-01-2013/SHARED ROOTS; South African Research Chair in PTSD from the Department of Science and Technology and the National Research Foundation; US Department of Defence Grant W81XWH08-2-0159 (PI: Stein, Murray B); VA RR&D I01RX000622; CDMRP W81XWH-08-2-0038; South African Medical Research Council; NARSAD Young Investigator; K01 MH118428; Department of Defense award number W81XWH-12-2-0012; ENIGMA was also supported in part by NIH U54 EB020403 from the Big Data to Knowledge (BD2K) program; R56AG058854; R01MH116147; R01MH111671; P41 EB015922; 1R01MH110483; 1R21 MH098198; R01MH105355-01A. The views expressed in this article are those of the authors and do not necessarily reflect the position or policy of the Department of Veterans Affairs, the United States Government, or any other funding sources listed here.

References

- Shalev A, Liberzon I, Marmar C (2017): Post-Traumatic Stress Disorder. *New Engl J Med.* 376:2459–2469. [PubMed: 28636846]
- Lindemer ER, Salat DH, Leritz EC, McGlinchey RE, Milberg WP (2013): Reduced cortical thickness with increased lifetime burden of PTSD in OEF/OIF Veterans and the impact of comorbid TBI. *Neuroimage-Clin.* 2:601–611. [PubMed: 24179811]
- Mueller SG, Ng P, Neylan T, Mackin S, Wolkowitz O, Mellon S, et al. (2015): Evidence for disrupted gray matter structural connectivity in posttraumatic stress disorder. *Psychiat Res-Neuroim.* 234:194–201.
- Wrocklage KM, Averill LA, Cobb Scott J, Averill CL, Schweinsburg B, Trejo M, et al. (2017): Cortical thickness reduction in combat exposed U.S. veterans with and without PTSD. *Eur Neuropsychopharmacol.* 27:515–525. [PubMed: 28279623]
- Li SG, Huang XQ, Li LJ, Du F, Li J, Bi F, et al. (2016): Posttraumatic Stress Disorder: Structural Characterization with 3-T MR Imaging. *Radiology.* 280:537–544. [PubMed: 26928229]

6. Hu H, Sun YW, Su SS, Wang Y, Qiu YM, Yang X, et al. (2018): Cortical surface area reduction in identification of subjects at high risk for post-traumatic stress disorder: A pilot study. *Aust Nz J Psychiat.* 52:1084–1091.
7. Klabunde M, Weems CF, Raman M, Carrion VG (2017): The moderating effects of sex on insula subdivision structure in youth with posttraumatic stress symptoms. *Depress Anxiety.* 34:51–58. [PubMed: 27862643]
8. Gong GL, He Y, Chen ZJ, Evans AC (2012): Convergence and divergence of thickness correlations with diffusion connections across the human cerebral cortex. *Neuroimage.* 59:1239–1248. [PubMed: 21884805]
9. Alexander-Bloch A, Giedd JN, Bullmore ET (2013): Imaging structural co-variance between human brain regions. *Nat Rev Neurosci.* 14:322–336. [PubMed: 23531697]
10. Romero-Garcia R, Whitaker KJ, Vasa F, Seidlitz J, Shinn M, Fonagy P, et al. (2018): Structural covariance networks are coupled to expression of genes enriched in supragranular layers of the human cortex. *Neuroimage.* 171:256–267. [PubMed: 29274746]
11. Sun D, Davis SL, Haswell CC, Swanson CA, LaBar KS, Fairbank JA, et al. (2018): Brain Structural Covariance Network Topology in Remitted Posttraumatic Stress Disorder. *Frontiers in Psychiatry.* 9.
12. Sun DL, Haswell CC, Morey RA, de Bellis MD (2019): Brain structural covariance network centrality in maltreated youth with PTSD and in maltreated youth resilient to PTSD. *Dev Psychopathol.* 31:557–571. [PubMed: 29633688]
13. Sun DL, Peveril MR, Swanson CS, McLaughlin KA, Morey RA (2018): Structural covariance network centrality in maltreated youth with posttraumatic stress disorder. *J Psychiatr Res.* 98:70–77. [PubMed: 29294430]
14. Yun JY, Boedhoe PSW, Vriend C, Jahanshad N, Abe Y, Ameis SH, et al. (2020): Brain structural covariance networks in obsessive-compulsive disorder: a graph analysis from the ENIGMA Consortium. *Brain.* 143:684–700. [PubMed: 32040561]
15. Cauda F, Nani A, Manuello J, Premi E, Palermo S, Tatu K, et al. (2018): Brain structural alterations are distributed following functional, anatomic and genetic connectivity. *Brain.* 141:3211–3232. [PubMed: 30346490]
16. Roos A, Fouche JP, Stein DJ (2017): Brain network connectivity in women exposed to intimate partner violence: a graph theory analysis study. *Brain Imaging Behav.* 11:1629–1639. [PubMed: 27757819]
17. Greenberg MS, Tanev K, Marin MF, Pitman RK (2014): Stress, PTSD, and dementia. *Alzheimers Dement.* 10:S155–S165. [PubMed: 24924667]
18. Sherin JE, Nemeroff CB (2011): Post-traumatic stress disorder: the neurobiological impact of psychological trauma. *Dialogues Clin Neurosci.* 13:263–278. [PubMed: 22034143]
19. Katrinli S, Stevens J, Wani AH, Lori A, Kilaru V, van Rooij SJH, et al. (2020): Evaluating the impact of trauma and PTSD on epigenetic prediction of lifespan and neural integrity. *Neuropsychopharmacol.* 45:1609–1616.
20. Wolf EJ, Chen CD, Zhao X, Zhou ZW, Morrison FG, Daskalakis NP, et al. (2021): Klotho, PTSD, and advanced epigenetic age in cortical tissue. *Neuropsychopharmacol.* 46:721–730.
21. Miller MW, Lin AP, Wolf EJ, Miller DR (2018): Oxidative Stress, Inflammation, and Neuroprogression in Chronic PTSD. *Harvard Rev Psychiat.* 26:57–69.
22. Mehta ND, Stevens JS, Li ZH, Gillespie CF, Fani N, Michopoulos V, et al. (2020): Inflammation, reward circuitry and symptoms of anhedonia and PTSD in trauma-exposed women. *Soc Cogn Affect Neur.* 15:1046–1055.
23. Clausen AN, Fercho KA, Monsour M, Disner S, Salminen L, Haswell CC, et al. (2021): Assessment of brain age in posttraumatic stress disorder: Findings from the ENIGMA PTSD and brain age working groups. *Brain and Behavior.*
24. Liao W, Zhang Z, Mantini D, Xu Q, Wang Z, Chen G, et al. (2013): Relationship between large-scale functional and structural covariance networks in idiopathic generalized epilepsy. *Brain Connect.* 3:240–254. [PubMed: 23510272]
25. Zielinski BA, Gennatas ED, Zhou JA, Seeley WW (2010): Network-level structural covariance in the developing brain. *P Natl Acad Sci USA.* 107:18191–18196.

26. Wannan CMJ, Cropley VL, Chakravarty MM, Bousman C, Ganella EP, Bruggemann JM, et al. (2019): Evidence for Network-Based Cortical Thickness Reductions in Schizophrenia. *Am J Psychiat.* 176:552–563. [PubMed: 31164006]
27. Rakic P (1988): Specification of Cerebral Cortical Areas. *Science.* 241:170–176. [PubMed: 3291116]
28. Rakic P (2009): Evolution of the neocortex: a perspective from developmental biology. *Nat Rev Neurosci.* 10:724–735. [PubMed: 19763105]
29. Horton JC, Adams DL (2005): The cortical column: a structure without a function. *Philos Trans R Soc Lond B Biol Sci.* 360:837–862. [PubMed: 15937015]
30. Sanabria-Diaz G, Melie-Garcia L, Iturria-Medina Y, Aleman-Gomez Y, Hernandez-Gonzalez G, Valdes-Urrutia L, et al. (2010): Surface area and cortical thickness descriptors reveal different attributes of the structural human brain networks. *Neuroimage.* 50:1497–1510. [PubMed: 20083210]
31. Yang JJ, Kwon H, Lee JM (2016): Complementary Characteristics of Correlation Patterns in Morphometric Correlation Networks of Cortical Thickness, Surface Area, and Gray Matter Volume. *Sci Rep-Uk.* 6.
32. Flory JD, Yehuda R (2015): Comorbidity between post-traumatic stress disorder and major depressive disorder: alternative explanations and treatment considerations. *Dialogues Clin Neuro.* 17:141–150.
33. Schnack HG, van Haren NEM, Brouwer RM, Evans A, Durston S, Boomsma DI, et al. (2015): Changes in Thickness and Surface Area of the Human Cortex and Their Relationship with Intelligence. *Cereb Cortex.* 25:1608–1617. [PubMed: 24408955]
34. Wierenga LM, Langen M, Oranje B, Durston S (2014): Unique developmental trajectories of cortical thickness and surface area. *Neuroimage.* 87:120–126. [PubMed: 24246495]
35. First MB (2015): Structured Clinical Interview for the DSM (SCID). In: RLCaSO Lilienfeld, editor. *The Encyclopedia of Clinical Psychology*, pp 1–6.
36. Weathers FW, Bovin MJ, Lee DJ, Sloan DM, Schnurr PP, Kaloupek DG, et al. (2018): The Clinician-Administered PTSD Scale for DSM-5 (CAPS-5): Development and initial psychometric evaluation in military veterans. *Psychol Assess.* 30:383–395. [PubMed: 28493729]
37. Weathers FW, Keane TM, Davidson JR (2001): Clinician-administered PTSD scale: a review of the first ten years of research. *Depress Anxiety.* 13:132–156. [PubMed: 11387733]
38. Beck AT, Steer RA, Brown GK (1996): *Manual for the Beck Depression Inventory-II.* San Antonio, TX: Psychological Corporation.
39. Radloff LS (1977): The CES-D scale: A self report depression scale for research in the general population. *Applied Psychological Measurements.* 1:385–401.
40. Hamilton M (1980): Rating Depressive Patients. *J Clin Psychiat.* 41:21–24.
41. M. H (1960): A rating scale for depression. *Journal of Neurology, Neurosurgery and Psychiatry.* 23:56–62. [PubMed: 14399272]
42. Lovibond PF, Lovibond SH (1995): The structure of negative emotional states: comparison of the Depression Anxiety Stress Scales (DASS) with the Beck Depression and Anxiety Inventories. *Behav Res Ther.* 33:335–343. [PubMed: 7726811]
43. Kovacs M (1985): The Children's Depression, Inventory (CDI). *Psychopharmacol Bull.* 21:995–998. [PubMed: 4089116]
44. Wang X, Xie H, Chen T, Cotton AS, Salminen LE, Logue MW, et al. (2020): Cortical volume abnormalities in posttraumatic stress disorder: an ENIGMA-psychiatric genomics consortium PTSD workgroup mega-analysis. *Mol Psychiatr.*
45. Destrieux C, Fischl B, Dale A, Halgren E (2010): Automatic parcellation of human cortical gyri and sulci using standard anatomical nomenclature. *Neuroimage.* 53:1–15. [PubMed: 20547229]
46. Rosen AFG, Roalf DR, Ruparel K, Blake J, Seelaus K, Villa LP, et al. (2018): Quantitative assessment of structural image quality. *Neuroimage.* 169:407–418. [PubMed: 29278774]
47. Fortin JP, Cullen N, Sheline YI, Taylor WD, Aselcioglu I, Cook PA, et al. (2018): Harmonization of cortical thickness measurements across scanners and sites. *Neuroimage.* 167:104–120. [PubMed: 29155184]

48. Radua J, Vieta E, Shinohara R, Kochunov P, Quide Y, Green MJ, et al. (2020): Increased power by harmonizing structural MRI site differences with the ComBat batch adjustment method in ENIGMA. *Neuroimage*. 218:116956. [PubMed: 32470572]
49. Sun D, Rakesh G, Haswell CC, Logue M, Lexi Baird C, O'Leary BM, et al. (2021): A Comparison of Methods to Harmonize Cortical Thickness Measurements Across Scanners and Sites. *bioRxiv*.2021.2009.2022.461242.
50. He Y, Chen ZJ, Evans AC (2007): Small-world anatomical networks in the human brain revealed by cortical thickness from MRI. *Cereb Cortex*. 17:2407–2419. [PubMed: 17204824]
51. Benjamini Y, Hochberg Y (1995): Controlling the False Discovery Rate - a Practical and Powerful Approach to Multiple Testing. *J R Stat Soc B*. 57:289–300.
52. Crossley NA, Mechelli A, Scott J, Carletti F, Fox PT, McGuire P, et al. (2014): The hubs of the human connectome are generally implicated in the anatomy of brain disorders. *Brain*. 137:2382–2395. [PubMed: 25057133]
53. Shang J, Lui S, Meng Y, Zhu H, Qiu C, Gong Q, et al. (2014): Alterations in low-level perceptual networks related to clinical severity in PTSD after an earthquake: a resting-state fMRI study. *PLoS One*. 9:e96834. [PubMed: 24823717]
54. Koch SB, van Zuiden M, Nawijn L, Frijling JL, Veltman DJ, Olff M (2016): Aberrant Resting-State Brain Activity in Posttraumatic Stress Disorder: A Meta-Analysis and Systematic Review. *Depress Anxiety*. 33:592–605. [PubMed: 26918313]
55. Ke J, Zhang L, Qi R, Xu Q, Zhong Y, Liu T, et al. (2018): Typhoon-Related Post-Traumatic Stress Disorder and Trauma Might Lead to Functional Integration Abnormalities in Intra- and Inter-Resting State Networks: a Resting-State Fmri Independent Component Analysis. *Cell Physiol Biochem*. 48:99–110. [PubMed: 30001548]
56. Suo X, Lei D, Li K, Chen F, Li F, Li L, et al. (2015): Disrupted brain network topology in pediatric posttraumatic stress disorder: A resting-state fMRI study. *Hum Brain Mapp*. 36:3677–3686. [PubMed: 26096541]
57. Ross MC, Cisler JM (2020): Altered large-scale functional brain organization in posttraumatic stress disorder: A comprehensive review of univariate and network-level neurocircuitry models of PTSD. *Neuroimage-Clin*. 27.
58. Fenster RJ, Lebois LAM, Ressler KJ, Suh J (2018): Brain circuit dysfunction in post-traumatic stress disorder: from mouse to man. *Nat Rev Neurosci*. 19:535–551. [PubMed: 30054570]
59. DeVille DC, Kuplicki R, Stewart JL, Tulsa I, Aupperle RL, Bodurka J, et al. (2020): Diminished responses to bodily threat and blunted interoception in suicide attempters. *Elife*. 9.
60. Gvozdanovic G, Stampfli P, Seifritz E, Rasch B (2020): Structural brain differences predict early traumatic memory processing. *Psychophysiology*. 57:e13354. [PubMed: 30825218]
61. Nambodiri VMK, Otis JM, van Heeswijk K, Voets ES, Alghorazi RA, Rodriguez-Romaguera J, et al. (2019): Single-cell activity tracking reveals that orbitofrontal neurons acquire and maintain a long-term memory to guide behavioral adaptation. *Nat Neurosci*. 22:1110–1121. [PubMed: 31160741]
62. Maren S, Holmes A (2016): Stress and Fear Extinction. *Neuropsychopharmacol*. 41:58–79.
63. Morey RA, Haswell CC, Hooper SR, De Bellis MD (2016): Amygdala, Hippocampus, and Ventral Medial Prefrontal Cortex Volumes Differ in Maltreated Youth with and without Chronic Posttraumatic Stress Disorder. *Neuropsychopharmacol*. 41:791–801.
64. Sun D, Peverill MR, Swanson CS, McLaughlin KA, Morey RA (2018): Structural covariance network centrality in maltreated youth with posttraumatic stress disorder. *J Psychiatr Res*. 98:70–77. [PubMed: 29294430]
65. Michopoulos V, Powers A, Gillespie CF, Ressler KJ, Jovanovic T (2017): Inflammation in Fear- and Anxiety-Based Disorders: PTSD, GAD, and Beyond. *Neuropsychopharmacol*. 42:254–270.
66. Wellman CL, Bollinger JL, Moench KM (2020): Effects of stress on the structure and function of the medial prefrontal cortex: Insights from animal models. *Int Rev Neurobiol*. 150:129–153. [PubMed: 32204829]
67. Godar SC, Bortolato M, Richards SE, Li FG, Chen K, Wellman CL, et al. (2015): Monoamine Oxidase A is Required for Rapid Dendritic Remodeling in Response to Stress. *Int J Neuropsychopharmacol*. 18.

68. Liston C, McEwen BS, Casey BJ (2009): Psychosocial stress reversibly disrupts prefrontal processing and attentional control. *Proc Natl Acad Sci U S A.* 106:912–917. [PubMed: 19139412]
69. Yeshurun S, Hannan AJ (2019): Transgenerational epigenetic influences of paternal environmental exposures on brain function and predisposition to psychiatric disorders. *Mol Psychiatry.* 24:536–548. [PubMed: 29520039]
70. Vukojevic V, Kolassa IT, Fastenrath M, Gschwind L, Spalek K, Milnik A, et al. (2014): Epigenetic modification of the glucocorticoid receptor gene is linked to traumatic memory and post-traumatic stress disorder risk in genocide survivors. *J Neurosci.* 34:10274–10284. [PubMed: 25080589]
71. Zannas AS, Provencal N, Binder EB (2015): Epigenetics of Posttraumatic Stress Disorder: Current Evidence, Challenges, and Future Directions. *Biol Psychiatry.* 78:327–335. [PubMed: 25979620]
72. Tozzi L, Farrell C, Booij L, Doolin K, Nemoda Z, Szyf M, et al. (2018): Epigenetic Changes of FKBP5 as a Link Connecting Genetic and Environmental Risk Factors with Structural and Functional Brain Changes in Major Depression. *Neuropsychopharmacol.* 43:1138–1145.
73. Raj A, LoCastro E, Kuceyeski A, Tosun D, Relkin N, Weiner M, et al. (2015): Network Diffusion Model of Progression Predicts Longitudinal Patterns of Atrophy and Metabolism in Alzheimer's Disease. *Cell Rep.* 10:359–369. [PubMed: 25600871]
74. Schmidt R, de Reus MA, Scholtens LH, van den Berg LH, van den Heuvel MP (2016): Simulating disease propagation across white matter connectome reveals anatomical substrate for neuropathology staging in amyotrophic lateral sclerosis. *Neuroimage.* 124:762–769. [PubMed: 25869856]
75. Villain N, Desgranges B, Viader F, de la Sayette V, Mezenge F, Landeau B, et al. (2008): Relationships between hippocampal atrophy, white matter disruption, and gray matter hypometabolism in Alzheimer's disease. *Journal of Neuroscience.* 28:6174–6181. [PubMed: 18550759]
76. Cafiero R, Brauer J, Anwander A, Friederici AD (2019): The Concurrence of Cortical Surface Area Expansion and White Matter Myelination in Human Brain Development. *Cereb Cortex.* 29:827–837. [PubMed: 30462166]
77. Dennis EL, Disner SG, Fani N, Salminen LE, Logue M, Clarke EK, et al. (2019): Altered white matter microstructural organization in posttraumatic stress disorder across 3047 adults: results from the PGC-ENIGMA PTSD consortium. *Mol Psychiatry.*
78. Seeley WW, Crawford RK, Zhou J, Miller BL, Greicius MD (2009): Neurodegenerative diseases target large-scale human brain networks. *Neuron.* 62:42–52. [PubMed: 19376066]
79. Lyall AE, Shi F, Geng X, Woolson S, Li G, Wang L, et al. (2015): Dynamic Development of Regional Cortical Thickness and Surface Area in Early Childhood. *Cereb Cortex.* 25:2204–2212. [PubMed: 24591525]
80. Geschwind DH, Rakic P (2013): Cortical evolution: judge the brain by its cover. *Neuron.* 80:633–647. [PubMed: 24183016]
81. Im K, Lee JM, Lyttelton O, Kim SH, Evans AC, Kim SI (2008): Brain size and cortical structure in the adult human brain. *Cereb Cortex.* 18:2181–2191. [PubMed: 18234686]
82. Panizzon MS, Fennema-Notestine C, Eyer LT, Jernigan TL, Prom-Wormley E, Neale M, et al. (2009): Distinct Genetic Influences on Cortical Surface Area and Cortical Thickness. *Cereb Cortex.* 19:2728–2735. [PubMed: 19299253]
83. Grasby KL, Jahanshad N, Painter JN, Colodro-Conde L, Bralten J, Hibar DP, et al. (2020): The genetic architecture of the human cerebral cortex. *Science.* 367:1340–+.
84. Suh JS, Schneider MA, Minuzzi L, MacQueen GM, Strother SC, Kennedy SH, et al. (2019): Cortical thickness in major depressive disorder: A systematic review and meta-analysis. *Prog Neuro-Psychoph.* 88:287–302.
85. Kroes MCW, Rugg MD, Whalley MG, Brewin CR (2011): Structural brain abnormalities common to posttraumatic stress disorder and depression. *J Psychiatr Neurosci.* 36:256–265.
86. Campbell DG, Felker BL, Liu CF, Yano EM, Kirchner JE, Chan D, et al. (2007): Prevalence of depression-PTSD comorbidity: Implications for clinical practice guidelines and primary care-based interventions. *J Gen Intern Med.* 22:711–718. [PubMed: 17503104]
87. Nijdam MJ, Gersons BPR, Olf M (2013): The role of major depression in neurocognitive functioning in patients with posttraumatic stress disorder. *Eur J Psychotraumatol.* 4.

88. Ramsawh HJ, Fullerton CS, Mash HBH, Ng THH, Kessler RC, Stein MB, et al. (2014): Risk for suicidal behaviors associated with PTSD, depression, and their comorbidity in the US Army. *J Affect Disorders*. 161:116–122. [PubMed: 24751318]
89. Ingalhalikar M, Smith A, Parker D, Satterthwaite TD, Elliott MA, Ruparel K, et al. (2014): Sex differences in the structural connectome of the human brain. *P Natl Acad Sci USA*. 111:823–828.

Author Manuscript

Author Manuscript

Author Manuscript

Author Manuscript

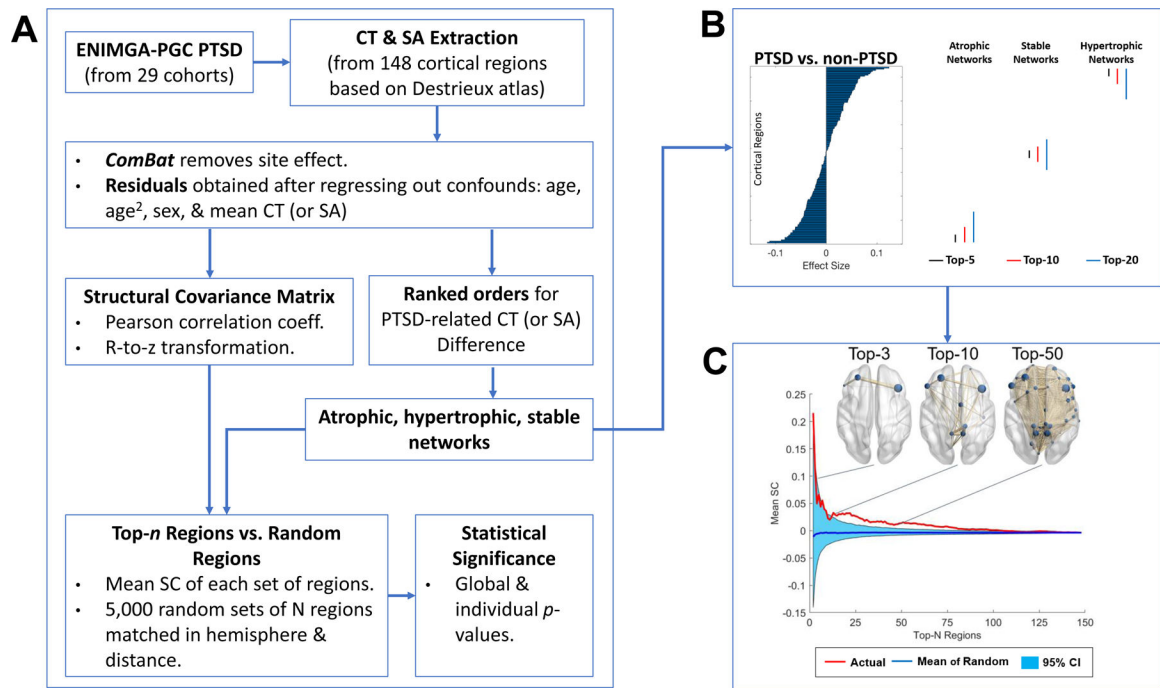


Figure 1. Analyses pipelines.

(A) Anatomical neuroimaging data from 29 research sites was aggregated by the ENIGMA PGC PTSD working group. Regional estimates of cortical thickness (CT) and surface area (SA) extracted from 148 cortical regions based on the Destrieux atlas (Destrieux, Fischl, Dale, & Halgren, 2010) were harmonized to remove site effects with *ComBat* approach and entered into a linear model to adjust for effects of age, age², sex, and whole-brain mean CT (or SA). The residuals were used to compute Pearson correlation coefficients for each pair of cortical regions across subjects within groups. The correlation coefficients were *r*-to-*z* transformed to improve normality and yielded a structural covariance (SC) matrix for each participant group. The cortical regions were rank ordered according to the magnitude of effect size when contrasting CT (or SA) between PTSD and non-PTSD groups. The top-*n* ($n = 2$ to 148) regions with the largest effect size of differences for PTSD > non-PTSD constituted atrophic networks, PTSD < non-PTSD constituted hypertrophic networks, while the smallest effect size stable networks. The mean SC of a given *n*-region network measured by the mean of positive correlations between all possible pairs of regions were compared to 5,000 randomly generated *n*-region networks matched for hemisphere and distance. Both global and individual tests were employed to compute statistical significance based on the proportion of mean SC values from randomly chosen sets of *n* regions that exceeded or equaled the mean SC of the actual top-*n* network. As illustrated in (B), the top-*n* ($n = 5, 10, \text{ and } 20$) regions showed (i) the largest effect size in CT (or SA) for PTSD < non-PTSD (atrophic networks); (ii) the largest effect size of PTSD > non-PTSD (hypertrophic networks); or (iii) the smallest effect size of PTSD vs. non-PTSD (stable networks). (C) CT-based hypertrophic networks for top-3, top-10 and top-50 regions.

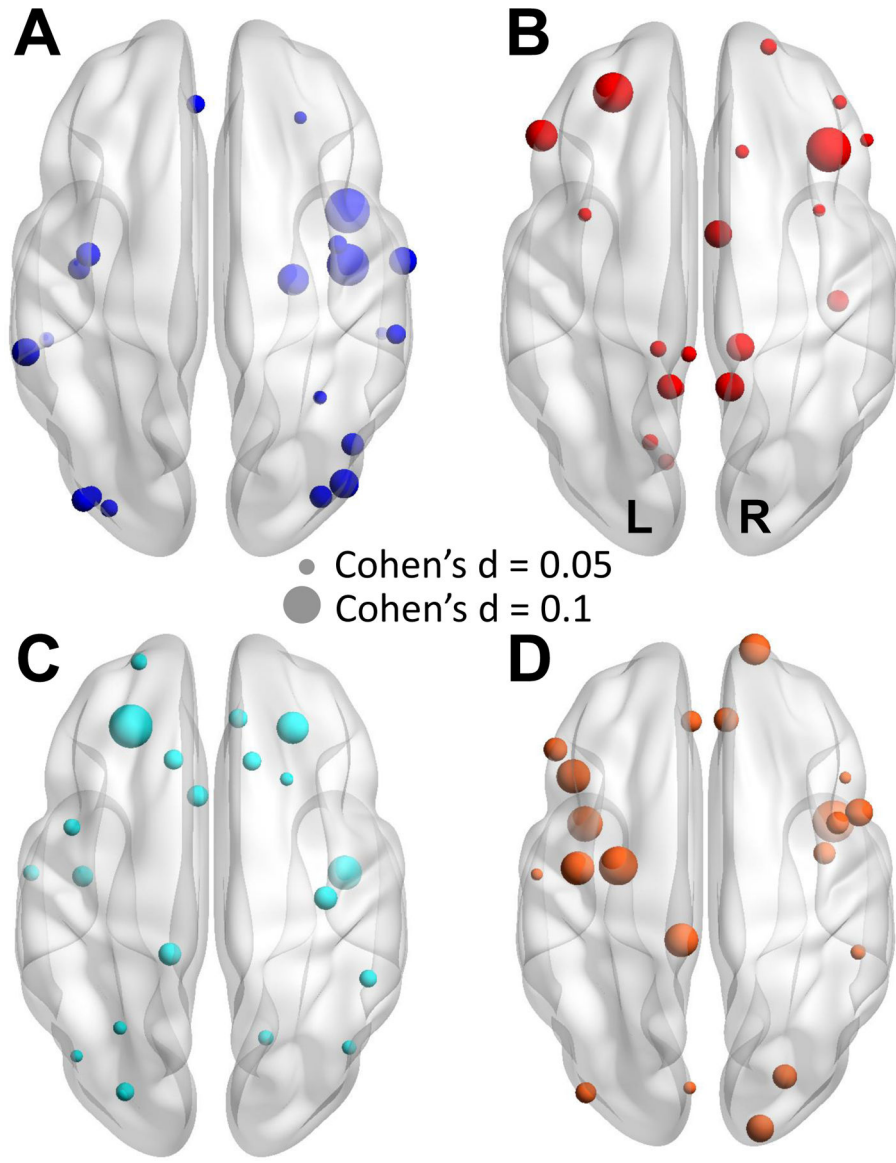


Figure 2. The top-20 regions showing PTSD-related differences. The top-20 regions that (A) PTSD < non-PTSD and (B) PTSD > non-PTSD in cortical thickness. The top-20 regions that (C) PTSD < non-PTSD and (D) PTSD > non-PTSD in surface area. Node size represents the magnitude of effect size for between-group differences per region. Warm color denotes PTSD > non-PTSD, and cool color denotes PTSD < non-PTSD. Regions names are listed in Supplementary Table S4. Two examples are shown on the right to denote the node size and the corresponding effect size (Cohen's d). The directions of the brain maps (axial view) are also shown.

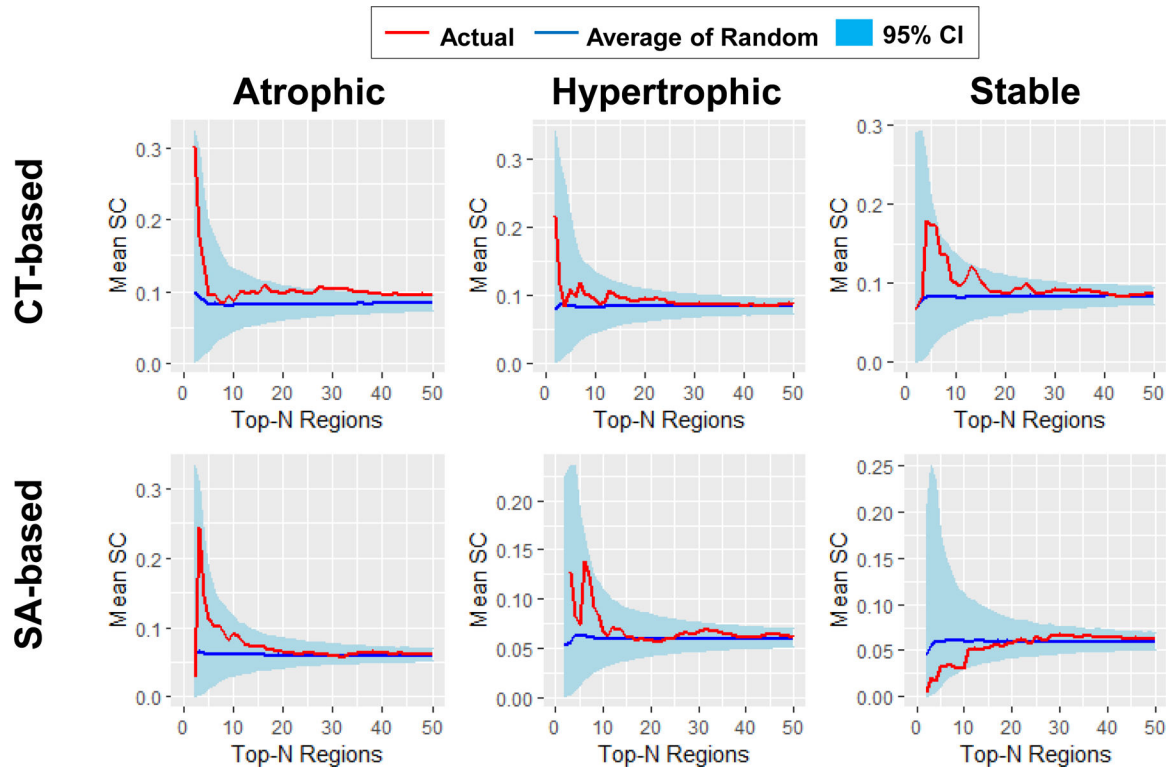


Figure 3. Mean SC of patients with PTSD.

Global tests showed that PTSD patients have higher mean SC in both CT- ($p < 0.001$) and SA-based ($p = 0.017$) atrophic networks, both CT- ($p = 0.029$) and SA-based ($p = 0.017$) hypertrophic networks, and CT-based ($p < 0.001$) but not SA-based ($p > 0.5$) stable networks than the corresponding random networks. The curves of networks with up to 50 nodes are shown for illustrative purposes, given that the mean SC of actual networks and the mean SC of the average of random networks were very similar for large network sizes. Red curve, mean SC of the actual networks; Blue curve, mean SC of the average of 5,000 random networks; light blue ribbon, 95% confidence interval (CI) of the 5,000 random networks.

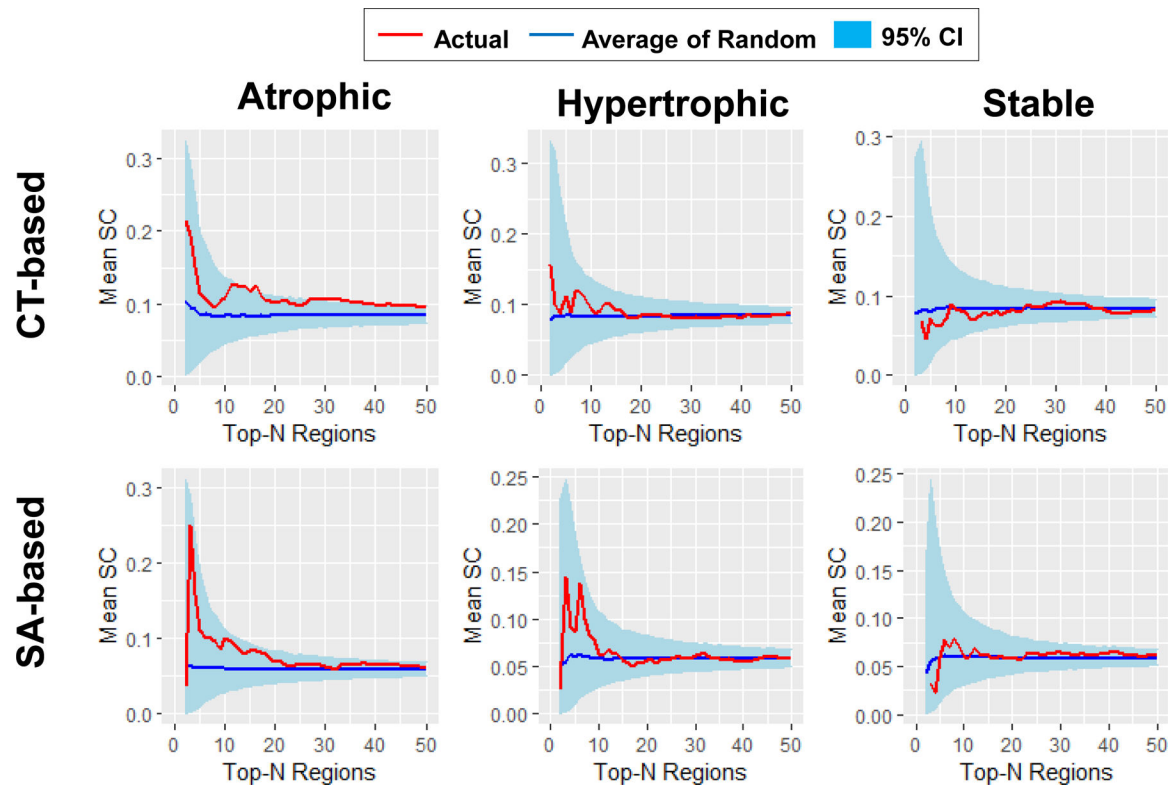


Figure 4. Mean SC of trauma-exposed participants without PTSD.

Global tests showed that participants without PTSD had higher mean SC in both CT- ($p < 0.001$) and SA-based ($p < 0.001$) atrophic networks, SA-based ($p = 0.014$) but not CT-based ($p = 0.139$) hypertrophic networks, and neither CT- ($p = 0.264$) nor SA-based ($p = 0.732$) stable networks than in corresponding random networks. The curves for networks with up to 50 nodes are shown for illustrative purpose, given that the mean SC of actual networks and the mean SC of the average of random networks were very similar for large network sizes. Red curve, mean SC of the actual networks; Blue curve, mean SC of the average of 5,000 random networks; light blue ribbon, 95% confidence interval (CI) of the 5,000 random networks.

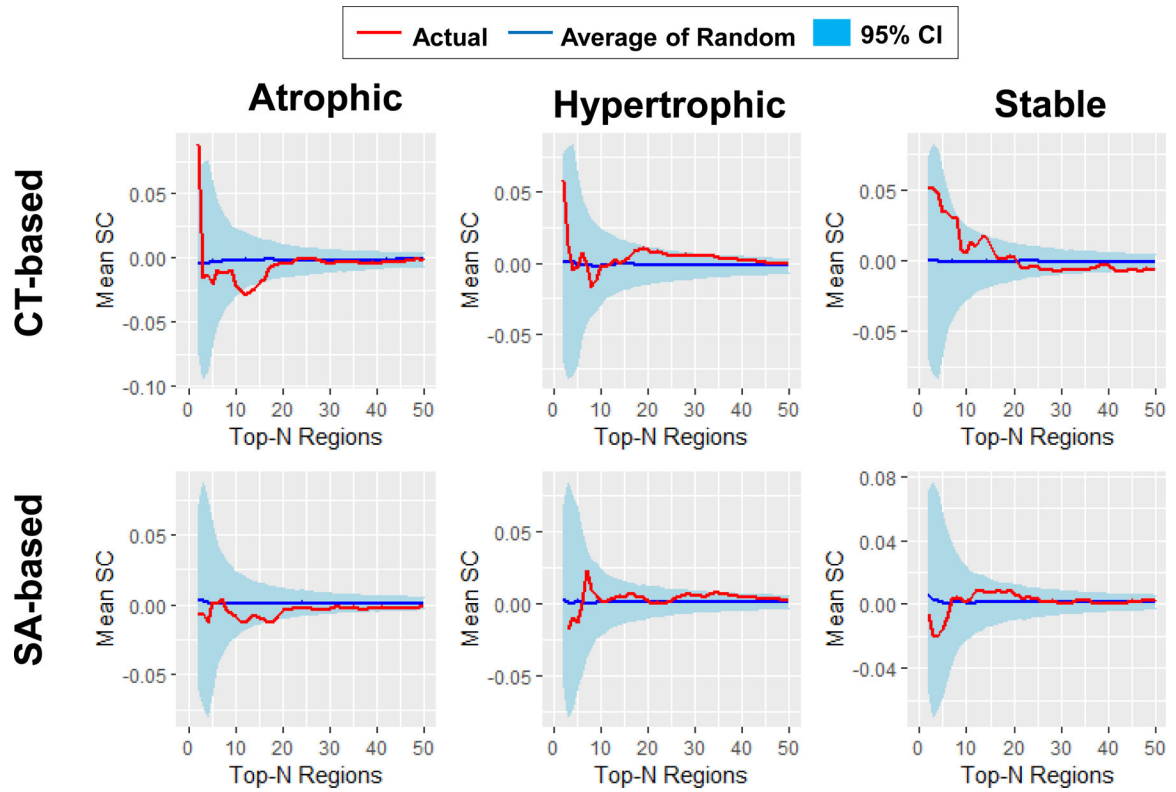


Figure 5. Mean SC of PTSD vs. non-PTSD.

Global tests showed that patients with PTSD versus non-PTSD participants had lower mean SC in both CT- ($p = 0.014$) and SA-based ($p = 0.024$) atrophic networks, but no significant difference in CT- ($p = 0.098$) and SA-based ($p > 0.5$) hypertrophic networks as well as CT- ($p > 0.5$) and SA-based ($p > 0.5$) stable networks. The curves of networks with up to 50 nodes are shown for illustrative purpose, given that the mean SC of actual networks and the mean SC of the average of random networks were very similar for large network sizes. Red curve, mean SC of the actual networks; Blue curve, mean SC of the average of 5,000 random networks; light blue ribbon, 95% confidence interval (CI) of the 5,000 random networks.

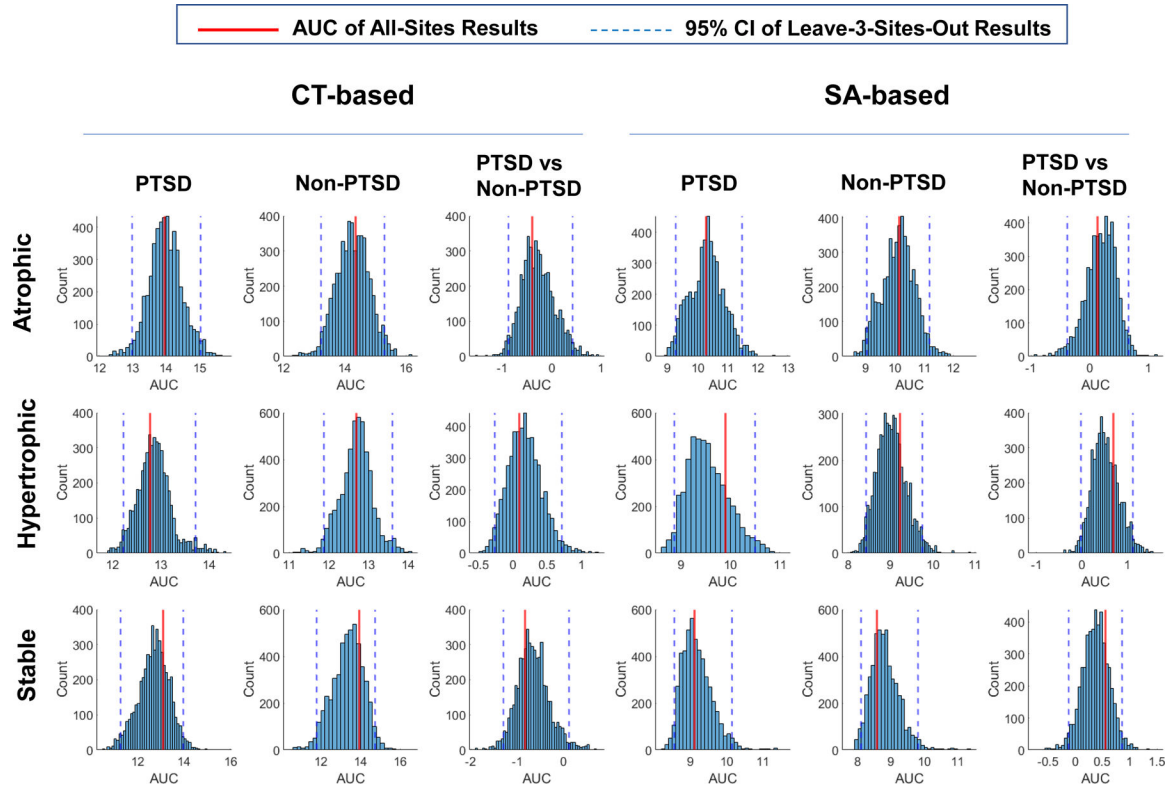


Figure 6. Replication analyses results.

The global-tests results shown in Figures 3, 4, and 5 are reliable as underscored by the area under curve (AUC) of mean SC for the results based on all 29 sites (represented by the red vertical line) was always located within the 95% confidence interval (represented by two blue vertical dashed lines) of the AUC of mean SC from 5,000 iterations leaving out 3 sites at each iteration across all types of networks.

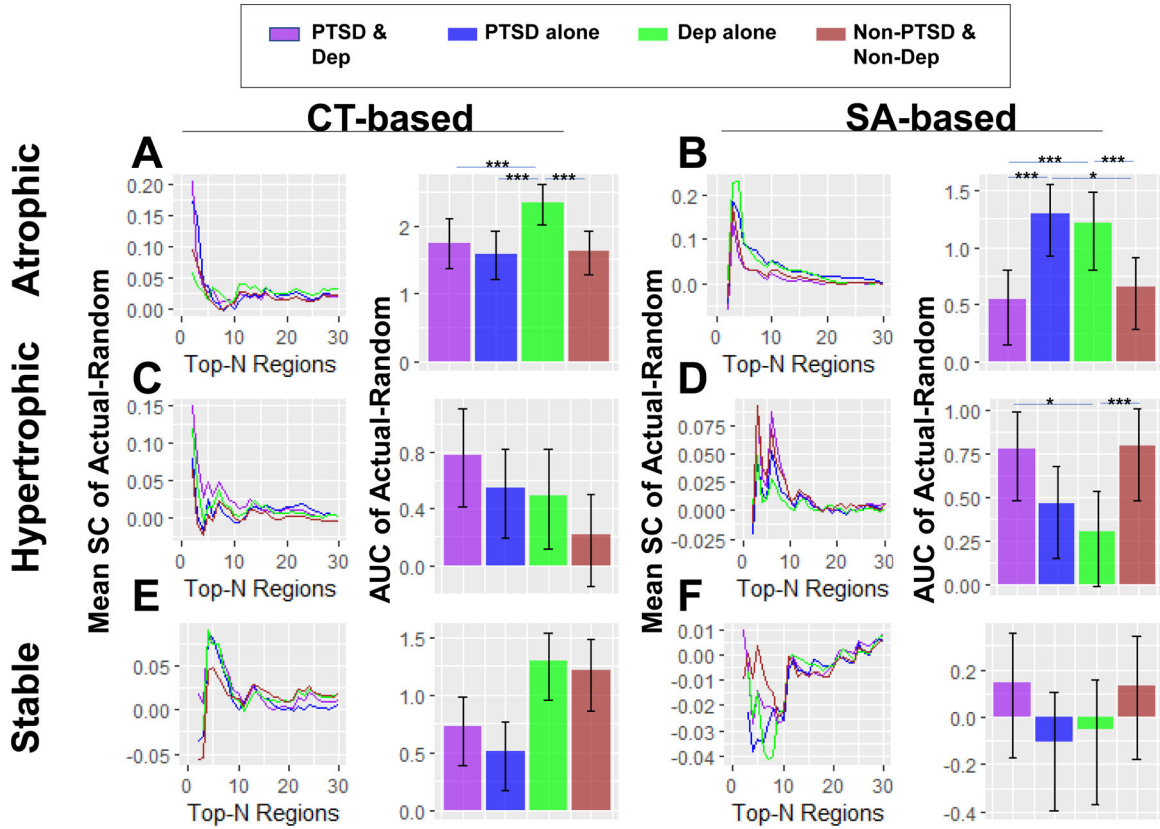


Figure 7. Interaction effects of PTSD and depression.

Global tests showed that patients with depression alone had higher mean SC in (A) CT-based ($p < 0.001$) and (B) SA-based ($p < 0.001$) atrophic networks, and lower mean SC in (D) SA-based hypertrophic networks ($p = 0.029$), than patients with both PTSD and depression. Patients with depression alone also showed higher mean SC in both (A) CT-based ($p < 0.001$) and (B) SA-based ($p < 0.001$) atrophic networks, and lower mean SC in (D) SA-based hypertrophic networks ($p < 0.001$), than patients with neither PTSD nor depression. Patients with PTSD alone showed lower mean SC in (A) CT-based atrophic networks than patients with depression alone ($p < 0.001$), and higher mean SC in (B) SA-based atrophic networks than patients with both PTSD and depression ($p < 0.001$) as well as participants with neither PTSD nor depression ($p = 0.014$). No significant PTSD x depression interaction effect (global p -values > 0.2) was found in the other types of networks shown in (C), (E) and (F). The curves of networks with up to 30 nodes were shown for illustrative purposes. Error bar denotes 95% confidence interval of 5,000 random networks. * represents $p < 0.05$; *** represents $p < 0.001$.

Table 1.

Demographic and clinical information per site.

Site	Number of Participants				Age (years)	Trauma	MDD (%)	Type
	CT	SA	Male/Female	PTSD/non-PTSD				
ADNIDOD	194	194	193/1	80/106	69.0±5	Y	2.5	Military
Booster (AMC)	75	75	40/35	38/37	40.0±10.0	Y	31	Police
Columbia	88	88	31/57	53/35	36.0±9.8	Y	24	Civilian
Duke University (DeBellis)	115	117	53/62	29/86	10.0±2.6	Y/N	N/A	Civilian
Minneapolis VAMC	169	171	161/8	74/95	33.0±7.9	Y	28.4	Military
Duke University/Durham VA	385	385	310/75	114/270	40.0±10.0	Y	40.3	Both
Ghent	67	67	0/67	8/59	37.0±12.0	N	46.3	Civilian
Groningen (Charité Berlin)	40	40	0/40	40/0	38.0±10.0	Y	67.5	Civilian
University of Wisconsin (Grupe)	57	58	53/4	19/38	31.0±6.4.0	Y	100	Military
Emory GTP	174	174	5/169	66/108	38.0±13.0	Y	51.7	Civilian
INTRUST	373	373	220/145	109/262	35.0±14.0	Y	21.7	Both
University of Wisconsin (Larson)	67	67	33/34	20/47	33.0±11.0	Y	0	Civilian
Leiden	52	52	7/45	22/30	15.2±2.0	N	19.2	Civilian
Mannheim	48	48	0/48	48/0	36.0±12.0	Y	97.9	Civilian
McLean	52	52	0/52	39/13	38.0±12.0	Y	75	Civilian
Muenster	47	47	5/42	21/26	27.0±7.0	Y	34	Civilian
Phan	43	43	43/0	23/20	32.0±8.0	Y	53.5	Military
McLean (Rosso)	106	97	49/57	21/85	34.0±9.0	Y	23	Civilian
University of Toledo	76	76	42/34	15/61	35.0±11.3	Y	41	Both
UCAS	70	70	32/38	34/36	50.0±7.0	Y	64.3	Civilian
Cape Town	62	63	0/62	7/55	29.0±8.0	Y	50	Civilian
University of Washington	255	255	125/130	53/202	14.0±3.1	Y	15.3	Civilian
WACO VA	66	66	56/10	41/25	41.0±11.1	N	67	Military
WestHaven VA	72	71	63/8	34/40	35.0±10.0	Y	75	Military
Yale	70	70	59/11	22/48	29.2±9.2	Y	0	Civilian
UNSW	162	163	63/99	49/113	40.4±8.0	Y	28.4	Civilian
South Dakota	123	123	99/24	78/45	29.0±7.0	Y	35	Both
Stellenbosch	260	260	72/188	121/139	41.0±13.0	Y	0	Civilian
Stanford	71	71	29/41	70/1	37.0±11.3	Y	0	Civilian
Total	3438	3436	1843/1586	1350/2076	-	-	29.9	-

Note: CT = cortical thickness; SA = surface area; Trauma = whether the non-PTSD participants are trauma-exposed; MDD (%) = percentage of participants who have major depressive disorder; Type = participants are from military/police, civilian, or both units.

Table 2.

Area under curve (AUC) of mean SC for the actual network and the average of 5,000 random networks.

Network Type	CT-based networks				SA-based networks			
	Act.	Rand.	.95 CI	Global p	Act.	Rand.	.95 CI	Global p
<i>PTSD</i>								
Atrophic	13.975	12.195	[11.918, 12.572]	<0.001 ^{***}	9.480	8.725	[8.494, 9.126]	0.017 [*]
Hypertrophic	12.846	12.104	[11.839, 12.512]	0.029 [*]	9.356	8.692	[8.483, 9.061]	0.017 [*]
Stable	13.211	12.193	[11.938, 12.567]	<0.001 ^{***}	8.652	8.689	[8.473, 9.049]	>0.500
<i>non-PTSD</i>								
Atrophic	14.483	12.397	[12.112, 12.785]	<0.001 ^{***}	9.616	8.511	[8.286, 8.918]	<0.001 ^{***}
Hypertrophic	12.832	12.317	[12.049, 12.729]	0.139	9.050	8.450	[8.242, 8.804]	0.014 [*]
Stable	11.977	12.260	[11.983, 12.642]	0.264	8.798	8.566	[8.363, 8.890]	0.732
<i>PTSD versus non-PTSD</i>								
Atrophic	-0.507	-0.205	[-0.382, -0.037]	0.014 [*]	-0.136	0.211	[0.052, 0.372]	0.024 [*]
Hypertrophic	0.015	-0.212	[-0.390, -0.037]	0.098	0.332	0.240	[0.079, 0.403]	>0.500
Stable	-0.155	-0.141	[-0.312, 0.033]	>0.500	0.172	0.215	[0.062, 0.376]	>0.500

Note: Act. = mean SC of the actual network; Rand. = average of the mean SC of 5,000 random networks; .95 CI = 95% confidence interval of the mean SC of 5,000 random networks; Global p = global *p* value (Bonferroni corrected) for the actual-versus-random comparison.

* , *p* < 0.05;

*** , *p* < 0.001.